Biochemical analysis of telomeric repeat binding factor 1

Biochemical analysis of telomeric repeat binding factor 1

BY

KAJAPARAN JEYANTHAN B.Sc. (Hons.)

A Thesis

Submitted to the School of Graduate Studies

In Partial Fulfillment of the Requirements

For the Degree

Master of Science

McMaster University

MASTER OF SCIENCE (2012) McMaster University

(Biology) Hamilton Ontario

TITLE	Biochemical analysis of telomeric repeat binding factor 1
AUTHOR	Kajaparan Jeyanthan, B.Sc. (McMaster University)
SUPERVISOR	Professor Xu-Dong Zhu
NUMBERS OF PAGES	xiii, 91

Abstract

TRF1 is an essential shelterin protein that binds to double stranded telomeric DNA. TRF1 is best known for its role as a negative regulator of telomere length. TRF1 has also been identified to play an important role in cell cycle regulation and DNA damage response. Post-translational modifications, like phosphorylation, have been shown to regulate TRF1 function in cells. Mass spectrometric analysis revealed three potential TRF1 phosphorylation sites, threonine 271, serine 279 and threonine 305 *in vivo*. To analyze the function of these three potential phosphorylation sites, phosphomimic (aspartic acid, D) and non-phosphorylatable (alanine, A) mutations were made to be analyzed *in vitro*. The recombinant phosphorylation mutants were analyzed through two different electrophoretic mobility shift assay conditions. Through *in vitro* gel shift assays, the phosphomimic mutation at threonine 271 mutant exhibits a DNA binding defect, whereas serine 279 and threonine 305 mutants have no binding defects. However, *in vivo* analysis needs to be conducted in order to determine whether this binding defect is authentic.

PIN2 is a TRF1 isoform, which is identical in its protein sequence with the exception of 20 amino acids (residue 296-316 of TRF1). The second study looks to characterize any potential functional differences between PIN2 and TRF1. *In vitro*, CDK1 kinase assay was conducted on TRF1 and PIN2 mutants to assess whether there was a difference in phosphorylation. The kinase assay revealed that both PIN2 threonine 351 and TRF1 threonine 371 are both phosphorylated by CDK1. However, the net phosphorylation level of PIN2 by CDK1 is far lower than the net phosphorylation level of

TRF1. An *in vitro* gel shift assay was also conducted to analyze the binding difference between TRF1 threonine 371 and PIN2 threonine 351 mutants. The DNA binding assay revealed that TRF1 threonine 371D mutant has a binding defect, whereas PIN2 threonine 351D mutant has no binding defect. These data suggest that PIN2 modification at the same site as TRF1 may behave differently. However, this data needs to be verified to determine whether a PIN2 threonine 351D mutant behaves like a phosphomimic.

Acknowledgements

I would like to first thank Dr. Xu-Dong Zhu for taking me in as her graduate student and for guiding me in the field of telomere research. Dr. Zhu has taught me the importance of critical thinking in research. Dr. Zhu is a passionate researcher. She has spent an enormous amount of her personal time assisting me with protocols like tissue culturing, and plasmid cloning. She always had her door open for discussion. She constantly challenged me throughout my thesis to improve my abilities, and encouraged me to stay in science. I will always remember the times that we spent together discussing ideas and coming up with potential models in the lab.

I would also like to thank my committee member Dr. Murray Junop. I appreciate all of your time and critical inputs. I have become a well rounded researcher because of the insight that you have provided me from a different point of view.

In addition, I am also grateful to my lab members. They have provided me companionship and some entertainment in the lab. However, I will remember them most for their assistance in trouble shooting and discussion about science. Also, I would like to thank the other students, faculty member and staff in the department who I had the opportunity to know.

I would also like to thank the Ontario government for awarding me with the Ontario Graduate scholarship which financially funded me during my second and third year of my masters.

Lastly, I would like to thank the support of my family. They have been cheering me on since day one.

Table of Contents

List of Figures

Abbreviations

A	Alanine
ADP	Adenosine diphosphate
ALT	Alternative lengthening of Telomere
AP	Alkaline phosphatase
ATP	Adenosine triphosphate
ATM	Ataxia telangiectasia mutated
ATR	Ataxia telangiectasia RAD3-related
BLM	Bloom's syndrome
BP	Base Pair
BSA	Bovine serum albumin
C-terminus	Carboxyl-terminus
CK	Casein Kinase
CDK	Cyclin-dependent kinase
D	Aspartic Acid
DNA	Deoxyribonucleic acid
DTT	Dithiothreitol
ECL	Enhanced chemiluminescence
EDTA	Ethylenediaminetetraacetic acid
EMSA	Electrophoretic Mobility Shift Assay
G	Guanine
HEPES	4-(2-hydroxyethyl)-1-piperazineethanesulfonic acid
hTERC	Human telomerase RNA component
hTERT	Human telomerase reverse transcriptase
IR	Ionizing radiation

KB	Kilobase
MOPS	3-(N-morpholino)-propanesulfonic acid
NHEJ	Non-homologous end joining
NT	Nucleotide
N-terminus	Amine-terminus
OB	Oligosaccharide/oligonucleotide binding
Oligo	oligonucleotide (pimers)
PAGE	Polyacrylamide gel electrophoresis
PARP	Poly (ADP-ribose) polymerase
PBS	Phosphate buffer saline
PCR	Polymerase chain reaction
PD	Population doubling
PMSF	Phenylmethylsulfonylfluoride
POT1	Protection of telomere 1
RTEL1	Regulator of telomere elongation helicase 1
S	Serine
SDS	Sodium dodecyl sulphate
SM	Silent mutant
T	Threonine
T-loop	Telomeric loop
TAE	Tris Acetate EDTA
TBE	Tris Borate EDTA
TIF	Telomere dysfunctional-induced foci
TIN2	TRF1 interacting nuclear protein 2
TPP1	TINT1/PTOP/PIP1
TRF	Telomere repeat binding factor

TRIS	2-amino-2-hydroxymethyl 1-1,3-propanediol
UV	Ultraviolet light
WT	Wild type

Chapter 1-Introduction

1.1 Telomeres

1.1.1 Telomere function in somatic cells

DNA is a macromolecule that contains genetic material which instructs the activity and function of all living organisms. Most prokaryotes and eukaryotic organelles contain a circular genome in which DNA replication results in no net loss of genetic information. In contrast, eukaryotic genomes are composed of linear chromosomes, which require end protection (Reviewed in Palm and de Lange, 2008).

During eukaryotic lagging strand DNA replication, Okazaki fragments are synthesized; each one requiring its own RNA primer (Okazaki *et al,* 1967). As one Okazaki fragment reaches an adjacent fragment, the adjacent RNA primer will be degraded and the resulting gap is filled in by DNA polymerase ε. As lagging strand synthesis approaches the end of a chromosome, the RNA primer at the extreme 5' end of the daughter strand will be degraded; however, the resulting gap is not replaced (Olovnikov, 1971). As a result, every subsequent round of replication leads to gradual shortening of DNA at the 3' end. This event is referred to as the end replication problem (Olovnikov, 1971; Watson, 1972; Olovnikov, 1973).

Telomeres are DNA-protein complexes located at the ends of linear eukaryotic chromosomes and they appear to be the solution to the end replication problem (Muller, 1938; McClintock, 1939; McClintock, 1941; Olovnikov, 1971; Watson, 1972; Blackburn

et al., 1978). Telomeres serve as a buffer between the distal genes and the shortening chromosomal ends. Human telomeres are made up of 2-20kb of TTAGGG tandem repeats (Meyne *et al.,* 1989; Cheng *et al.,* 1989; Moyzis *et al.,* 1988; de Lange *et al.,* 1990) and a 3' G-rich single strand overhang of 200 ± 75nt (Makarov *et al.,* 1997; McElligott *et al.,* 1997; Wright *et al.,* 1997; Wellinger and Sen, 1997) (Fig. 1.1A). In 1985, Elizabeth Blackburn, Jack Szostak and Carol Greider, pioneers in telomere research and nobel laureates, discovered telomerase (Szostak and Blackburn, 1982; Greider and Blackburn, 1985). Telomerase is a reverse transcriptase made up of an RNA subunit, TERC, and a protein catalytic subunit, TERT (Feng *et al.,* 1995; Harrington *et al.,* 1997; Kilian *et al.,* 1997; Nakamura *et al.,* 1997, Meyerson et al., 1997). This unique ribonucleoprotein is responsible for extending telomeric repeats *de novo* (Greider and Blackburn, 1985; Feng *et al.,* 1995; Nakamura *et al.,* 1997). However, in human somatic cells the protein component of telomerase, hTERT, is not expressed (Nakamura *et al.,* 1997; Bodnar *et al.,* 1998). As a result, every time somatic cells divide, telomeres shorten. Eventually, telomeres reach to a threshold that triggers cellular senescence, a state in which cells do not divide, but maintain metabolic function (Harley, 1991; Hayflick, 1965; Hayflick *et al.,* 1961). Unlike human somatic cells, stem cells and germline cells have telomerase activity (Broccoli et al., 1995; Kim et al., 1994; Chiu *et al.,* 1996). Interestingly, activation of telomerase is observed in most types of cancers, which indicates that telomere maintenance plays an important role in both cancer and cellular aging (Meyerson *et al.,* 1997; Counter, 1992).

The tandem sequence and structure of telomeres renders them vulnerable to DNA damage. The G-rich nature of telomeres makes them prone to oxidative damage resulting in DNA lesion products like 8-oxo-guanine (Oikawa *et al.*, 2001). Higher order DNA structures like G-quadruplexes can also form at telomeres resulting in DNA polymerase stalling during DNA replication (Sfier *et al.*, 2009; Martínez *et al.*, 2009; Vannier *et al.*, 2012). Additionally, the rich thymidine presence at telomeres makes these tandem sequences liable to the formation of pyramidine dimers when exposed to UV (Kruk *et al.*, 1995). Due to these characteristics, this region of the genome has a proportionately higher presence of repair complexes (Reviewed by Baumgartner *et al.*, 2005)

Interestingly, telomeres in an open confirmation state can be mistakenly recognized by DNA damage surveillance proteins as a double strand break. Some DNA repair systems like NHEJ may attempt to repair two unprotected ends at close proximity by fusing them together, leading to chromosomal fusions (Zhu *et al.*, 2003; Celli *et al.*, 2005; Soutogulou *et al.*, 2007; Konishi and de Lange, 2008). To prevent unnecessary repair from occurring at telomeres, an assembly of telomere-specific proteins known as the shelterin complex helps to form a higher order structure at telomere ends, known as the t-loop (Griffith *et al.*, 1999; Reviewed by de Lange, 2005). The t-loop structure is formed when the 3' telomere overhang loops backwards and invades upstream into double stranded telomeric DNA, binding to the complementary strand and displacing the other strand to form a D-loop (Griffith *et al.*, 1999) (Fig. 1.1B). The structural importance of the t-loop is postulated to sequester and hide the 3' G-rich overhang from being detected by repair surveillance proteins (Griffith *et al.*, 1999). It is also important to note

that t-loop resolution is necessary during certain times of the cell cycle, as a persistent t-loop structure can actively stall and block replication machineries from reaching the ends of chromosomes. This may result in fragile break sites and the removal of telomere ends through the formation of telomere circles by the SLX4 nuclease complex (Reviewed by Gilson *et al.,* 2007; Vannier *et al.,* 2012). The recruitment and inhibition of DNA repair proteins at telomeres is regulated by the shelterin complex (Reviewed by De Lange, 2005).

1.1.2 Shelterin Complex

The shelterin complex is made up of six proteins (TIN2, TPP1, POT1, TRF2, RAP1 and TRF1) that localize to telomeres (Fig. 1.1C). The six member complex is held together by TIN2, a multiple docking protein (Kim *et al.,* 1999; Kim *et al.,* 2004; Ye *et al.,* 2004b; O'Conner *et al.,* 2006). TIN2 directly binds to TRF1, TRF2 and TPP1, while RAP1 and POT1 bind through TRF2 and TPP1 respectively (Kim *et al.,* 1999; Houghtaling *et al.,* 2004; Kim *et al.,* 2004; Liu *et al.,* 2004; Ye *et al.,* 2004b; Ye *et al.,* 2004c; O'Conner *et al.,* 2006). RNA interference of TIN2 compromises the association of the other shelterin proteins with telomeres (Ye *et al.,* 2004b). TPP1 is known best for its recruitment of POT1 to the 3' G-rich overhang (Houghtaling *et al.,* 2004; Liu *et al.,* 2004; Ye *et al.,* 2004c). In addition, TPP1 has been shown to physically recruit telomerase to telomeres through its OB-fold domain (Zhong *et al.,* 2012; Xin *et al.,* 2007; Wang *et al.,* 2007). POT1 is a single stranded DNA binding protein that is specific to the 3' G-rich overhang (Baumann *et al.,* 2001; Lei *et al.,* 2004; Loayza *et al.,* 2004). POT1

protects the G-rich overhang from being identified by the ATR-mediated pathway as a site of damage (Denchi *et al.*, 2007). RAP1 is found on telomeres in a 1:1 ratio with TRF2, and it is implicated in inhibiting NHEJ with TRF2, which has been shown to occur *in vitro* regardless of the telomere structure order (t-loop or linear) (Li *et al.*, 2000; Zhu *et al.*, 2000; Sarthy *et al.*, 2009; Bae and Baumann, 2007). TRF2 binds to double stranded telomere DNA as a homodimer (Bilaud *et al.*, 1997; Broccoli et al., 1997; Fairall *et al.*, 2001). Knockdown of TRF2 results in end to end fusions of telomeres, an increase in telomere dysfunction-induced foci (TIF), and a reduction in the proliferation and viability of cells (van Steensel *et al.*, 1998; Karlseder *et al.*, 1999; Smogorzewska *et al.*, 2002; Celli *et al.*, 2005; Konishi *et al.*, 2008). TIFs, telomere induced foci, formed in the absence of TRF2 are produced by the activation of the ATM-mediated DNA damage response pathway, suggesting a role for TRF2 in repressing ATM activation at telomeres (Celli and de Lange, 2005; Karlseder *et al.*, 1999; Denchi and de Lange, 2007). TRF2 has also been shown to promote the formation of t-loop structures from telomere substrates *in vitro* (Stansel *et al.*, 2001).

1.2 TRF1

1.2.1 TRF1-Structure and Function

In 1992, TRF1 was isolated and identified through a telomeric elecotrophoretic mobility shift assay (EMSA) screen using HeLa extracts (Zhong *et al.*, 1992). TRF1 and TRF2 are believed to be paralogs due to their structural and domain sequence similarities. Both TRF1 and TRF2 have a TRFH domain (~30% similarities) and a C-terminal Myb-

like DNA binding domain (56% similarities) (Broccoli *et al.,* 1997; Bilaud *et al.,* 1997; Fairall *et al.,* 2001) (Fig. 1.2A). However, the two proteins differ mostly at the N-terminus where TRF1 has an acidic region and TRF2 has a basic region (Broccoli *et al.,* 1997; Bilaud *et al.,* 1997; Ancelin *et al.,* 1998) (Fig. 1.2A). It has been suggested through *in vitro* analysis, that the acidic region of TRF1 inhibits 3' overhang invasion as well as telomeric DNA condensation (Poulet *et al.,* 2012). This was elucidated through substituting the basic region of TRF2 with the acidic region of TRF1 which results in the repression of both strand invasion and telomeric DNA condensation (Poulet *et al.,* 2012). Similarly, deletion of the acidic region of TRF1 was able to promote 3' overhang strand invasion and induce telomeric DNA condensation (Poulet *et al.,* 2012). Like TRF2, TRF1 binds to double stranded telomeric DNA (Zhong *et al.,* 1992; Hanish *et al.,* 1994; Chong *et al.,* 1995). *In vitro* gel shift assays show that sequestering TRF1 monomers by increasing the concentration of TRF1ΔMyb monomers resulted in a weaker binding signal to telomeric substrates (Bianchi *et al.,* 1997). This experiment illustrates that TRF1 binds to telomeric DNA as a homodimer and that the Myb domain is responsible for TRF1 localizing to telomeric DNA. The deletion of the TRFH domain disrupts TRF1 localization to telomeres as it is responsible for homodimerization (Bianchi *et al.,* 1997). The TRFH domain also serves as a docking site for interacting partners that contain a Y/FxLxP sequence motif and recruits these proteins to telomeres (Chen *et al.,* 2008; Kim et al, 2009). TRF1 null mice die at E6.5, six days after fertilization. This observation indicates that TRF1 is an essential gene (Karlseder *et al.,* 2003).

TRF1 is best known for its role as a negative regulator of telomere length (van Steensel and de Lange 1997; Smogorzewska *et al.,* 2000; Ancelin *et al.,* 2002). A dominant negative mutation of TRF1 results in telomere elongation in telomerase positive cells (van Steensel and de Lange 1997). On the other hand, overexpression of TRF1 in telomerase positive cells results in telomere shortening (van Steensel and de Lange 1997). Southern blot analysis of TRF1 knockdown in HT1080 cells showed that there was a gradual elongation in telomere length consistent with telomerase-mediated length maintenance, ruling out the involvement of telomere lengthening by recombination (ALT Pathway - Alternative Lengthening of Telomeres) (van Steensel and de Lange 1997). It has been suggested that TRF1 blocks telomerase from binding to telomeres in *cis* (van Steensel and de Lange 1997; Smogorzewska *et al.,* 2000; Ancelin *et al.,* 2002) (Fig. 1.2B). A popular model was designed from this observation. The protein counting model concludes that longer telomeres have more bound TRF1, thus preventing further elongation and allowing for gradual telomere shortening (Smogorzewska *et al.,* 2000). However, shorter telomeres have less TRF1 localization and allow for telomerase access. This model is supported by the fact that cell lines expressing telomerase in the presence of shelterin proteins, like TRF1, appear to equilibrate and maintain telomere length with no gradual elongation or shortening (Smogorzewska *et al.,* 2000).

TRF1 deletion also causes a problem for the progression of replication forks at telomeres (Sfier *et al.,* 2009; Martínez *et al.,* 2009). The repetitive sequence of telomeres can form higher order structures that have the potential to cause replication fork and DNA polymerase stalling. Conditional TRF1 mice knockouts show the formation of

fragile telomere sites, which can arise from a defect in DNA replication (Sfier *et al.,* 2009). De Lange and Sfier show that BLM and RTEL1 knockdowns produce telomere phenotypes similar to those seen in the conditional TRF1 mice knockout (Sfier *et al.,* 2009). This led to a model that suggests that TRF1 recruits BLM and RTEL1 helicases to the replication fork to resolve any barriers at telomeres (Sfier *et al.,* 2009).

TRF1 is an abundant protein, 30-200 thousand copies in HeLa1.3 and HTC75 cells, which is highly regulated in a cell cycle dependent manner (Takai *et al.,* 2010; Shen *et al.,* 1997; Reviewed Walker *et al.,* 2012). One well characterized TRF1 modification is the poly ADP-ribosylation of TRF1 during sister telomere resolution in anaphase by tankyrase 1, a poly (ADP-ribose) polymerase (Dynek *et al.,* 2004; Smith *et al.,* 1998). Yeast two-hybrid analysis elucidated that tankyrase 1 interacts with TRF1 at its N-terminal acidic region (Smith *et al.,* 1998). *In vitro* gel shift and PARP assays revealed that tankyrase 1 ADP-ribosylates TRF1 resulting in the removal of TRF1 from telomeres (Smith *et al.,* 1998; Ye and Titia De Lange, 2004). Overexpression of tankyrase 1 results in reduced TRF1 levels and telomere elongation in telomerase positive cells (Smith and De Lange, 2000). The dimerization domain of TRF1 (TRFH) contains a destruction-like motif that is similar to the destruction box domain found in mitotic cyclins (Shen *et al.,* 1997). It has been documented that unbound TRF1 is subjected to ubiquitin mediated degradation (Chang *et al.,* 2003; Lee *et al.,* 2006). The ubiquitination of TRF1 is mediated by Fbx4, an F-box protein that acts as a substrate specific adaptor for ubiquitin E3 ligases (Lee *et al.,* 2006). Interestingly, overexpresssion of TRF1 causes entry into mitosis followed by apoptosis (Shen *et al.,* 1997). Kishi and colleagues showed an

increase in caspase 3 and other apoptotic markers in cell lines overexpressing TRF1 (Kishi *et al.,* 2001). Mutations in the Myb-like domain that abrogate TRF1 localization to telomeres failed to repress the apoptotic phenotype found in cell lines that were overexpressing TRF1 (Kishi *et al.,* 2001). This indicates that there may be a role for unbound TRF1. However, these TRF1 induced apoptotic events were reported to be exclusively seen in cell lines with short telomeres and need to be studied in further detail (Wu *et al.,* 2008). In addition to ADP-ribosylation and ubiquitination, phosphorylation has been shown to regulate TRF1 activity at telomeres.

1.2.2 TRF1 phosphorylation

TRF1 is subjected to phosphorylation by an array of kinases. This is possibly due to the presence of multiple serine and threonine residues. Antibodies specific to phosphoserine or phosphothreonine both detect TRF1 in cellular extracts (Wu *et al.,* 2007) (Fig. 1.2C; Table 1). Phosphorylation studies of TRF1 have revealed its importance in DNA damage response and cell cycle progression.

In response to ionizing radiation at telomeres, ATM phosphorylates TRF1 (Kishi *et al.,* 2001). ATM is a phosphatidylinositol 3-kinase-related protein that primarily responds to double strand breaks by activating downstream repair proteins (Reviewed by Palm *et al.,* 2008). ATM deficient (AT) cells undergo mitotic entry and apoptosis following IR treatment (Kishi *et al.,* 2002). In contrast, an ATM positive cell treated with IR would repair the double strand break then proceed to mitosis (Kishi *et al.,* 2002). AT cells also experience rapid telomere shortening when grown for an extended period of

time, suggesting complications in telomere stability (Kishi *et al.,* 2002). GST pull down assays using truncated recombinant TRF1 as bait revealed that the first 208aa are sufficient to physically interact with ATM (Kishi *et al.,* 2001). The physical interaction is necessary for ATM to phosphorylate TRF1 in response to DNA damage (Kishi *et al.,* 2001) (Fig. 1.2C; Table 1). Kun Ping Lu's group show that by abrogating TRF1 binding to telomeres, the apoptotic phenotype seen in AT cells was rescued in the presence of IR treatment (Kishi *et al.,* 2002). Interestingly, Wu and colleagues observed inhibition of ATM using KU59933 results in an increase in TRF1 binding to telomere via ChIP (Wu *et al.,* 2007). Two additional consensus ATM phosphorylation sites (S367 and S274) were analyzed (Wu *et al.,* 2007) (Fig. 1.2C; Table 1). Gel shift assays using phosphomimic mutants TRF1S367D and TRF1S274D show a decrease in binding to telomeric substrates compared to wild type control, whereas phosphomimic mutant TRF1S219D binding was equivalent to wild type TRF1 (Wu *et al.,* 2007). These results suggest a model in which ATM phosphorylates and removes TRF1 from telomeres (Wu *et al.,* 2007). The removal of TRF1 would allow for the access of telomerase to telomeres when replication forks are stalled (Wu *et al.,* 2007). This model helps provide an explanation for the rapid telomere shortening that AT cells experience (Wu *et al.,* 2007). In addition, negative regulation of TRF1 by ATM may allow for DNA repair to take place in response to IR (Kishi and Lu 2002).

TRF1 is also phosphorylated in a cell cycle dependent manner. The mitotic kinase Aurora-A phosphorylates TRF1-S296 during mitosis (Ohishi *et al.,* 2010) (Fig. 1.2C; Table 1). Overexpression of Aurora-A with endogenous TRF1 results in delayed

mitosis, multinucleated cells that contain irregular cell divisions and overall cytokinetic failure (Ohishi *et al.,* 2010). However, this cellular fate can be rescued by knocking down TRF1 or overexpressing tankyrase 1 (Ohishi *et al.,* 2010). Although the study did not elucidate a mechanism between the interaction of TRF1 and Aurora-A, the phenotypes suggest that TRF1 is involved in mitotic progression in human cells (Ohishi *et al.,* 2010). Interestingly, ATM was also identified to phosphorylate TRF1 independently of IR induced DNA damage response (McKerlie *et al.,* 2012). TRF1-S367 phosphorylation by ATM results in its disassociation from telomeres and the formation of distinct foci sensitive to protease inhibitors during S/G2-phase (McKerlie *et al.,* 2012) (Fig. 1.2C; Table 1). This unbound pool of phosphorylated TRF1 is targeted for protein degradation as observed in a cyclohexamide (protein biosynthesis inhibitor) treatment experiment (McKerlie *et al.,* 2012). Another mitotic kinase, Polo-like kinase 1 (PLK1), phosphorylates TRF1 at serine 435 in a cell cycle dependent manner (Wu *et al.,* 2008) (Fig. 1.2C; Table 1). Gel shift assays show that *in vitro* phosphorylation of TRF1-S435 resulted in a stronger binding to telomeric substrates compared with unphosphorylated TRF1 (Wu *et al.,* 2008). CDK1 phosphorylation of TRF1-T371 has been shown to sequester TRF1 from telomeres during mitosis which is required for sister telomere resolution during anaphase (McKerlie, 2011) (Fig. 1.2C; Table 1). *In vitro* gel shift assay and *in vivo* ChIP analysis showed that TRF1-T371D mutants have a reduced affinity towards telomeric DNA (McKerlie, 2011). Interestingly, unlike the phosphorylated S367 pool, this unbound pool of phosphorylated TRF1-T371 was not targeted for degradation and was more stable than the unphosphorylated TRF1 form (McKerlie, 2011).

Other TRF1 phosphorylation sites that promote DNA binding and protein stability have also been identified. CK2 has been identified to phosphorylate TRF1 at site T122 (Kim *et al.*, 2008). This TRF1 phosphorylation promotes DNA binding, which was observed through gel shift assays (Kim *et al.*, 2008) (Fig. 1.2C; Table 1). Cell lysates treated with phosphatase or CK2 inhibitors resulted in a decrease in Flag-TRF1 DNA complex formation via EMSA (Kim *et al.*, 2008). The reduction in DNA binding in T122A mutant is due to the fact that this mutation blocks TRF1 homo-dimerization. This finding was illustrated through a co-immunoprecipitation between RFP-TRF1 WT and Flag-TRF1-T122 mutants. CK2 knockdown resulted in ubiquitination of TRF1 and a reduction in endogenous TRF1 levels via western and IF, indicating that this phosphorylation site plays a role in protein stability (Kim *et al.*, 2008).

Another TRF1-interacting kinase, AKT, was identified through coimmunoprecipitation (Chen and Wu, 2009). AKT kinase, a serine/threonine kinase involved in cell proliferation and apoptosis, was identified to phosphorylate TRF1-T273 via *in vitro* kinase assay (Chen and Wu, 2009) (Fig. 1.2C; Table 1). Overexpression of AKT results in an increase of endogenous levels of TRF1 suggesting a role in protein stability (Chen and Wu, 2009). However, more studies are required to fully address AKT function at telomeres and its effect on TRF1 phosphorylation.

There remain several potential phosphoserine and phosphothreonine sites that may regulate the role of TRF1 at telomeres. This thesis project will look at three residues that are located in the linker region that connects the TRFH domain to the Myb-like

domain. These residues are T271, S279 and T305, all of which have been suggested to be candidate phosphorylation sites through mass spectrometry. However, the function of these phosphorylation sites has yet to be elucidated. Phosphomimic (aspartic acid) and non-phosphorylatable (alanine) mutants were generated for all three sites to help address the role of phosphorylation on each respective site. The objective of part one of my thesis was to determine whether any of these three TRF1 phosphorylation sites play a role in modulating TRF1 function at telomeres. The function of these residues will be focused through the use of *in vitro* gel shift assays.

The *in vitro* gel shift assay is a standard protocol used to quantify the level of protein bound to probe DNA (reviewed by Hellman *et al.,* 2007). In the telomere field, the *in vitro* gel shift assay revealed many important function and defining features of TRF1. The use of recombinant TRF1 in conjunction with gel shift assay was the first protocol performed to determine that TRF1 bound as a dimer, the Myb-like domain is the DNA binding domain of TRF1, and that TRF1 is a spatially flexible protein (Bianchi *et al.,* 1997; Bianchi *et al.,* 1999). *In vitro* gel shift assays were also used to help characterize a series of phospho-TRF1 sites (Wu e*t al.*, 2007; Kim et al., 2008; Wu *et al.*, 2008; McKerlie et al., 2011; McKerlie et al., 2012).

1.3 PIN2

In 1997, a TRF1 isoform, PIN2, was identified through a yeast two hybrid screening method using NIMA mitotic kinase as bait (Shen *et al.,* 1997). Protein sequence analysis revealed that PIN2 is identical to TRF1 with the exception of 20 amino

acids (residue 296-316 of TRF1) which are missing in the linker region of PIN2 (Shen *et al.,* 1997) (Fig.1.3). The alternative splicing of exon 8 from the same ORF of TRF1 produces the PIN2 mRNA (Lages *et al.,* 2004). The Kun Ping Lu group also observed that both PIN2 mRNA and protein levels were higher compared to the TRF1 isoform (Shen *et al.,* 1997). Pin2 binds to double stranded telomeric DNA and regulates telomere length in a manner indistinguishable from TRF1 (Shen *et al.,* 1997; Reviewed by Zhou *et al.,* 2003). Interestingly, there has yet to be any functional differences found between PIN2 and TRF1 (Reviewed by Zhou *et al.,* 2003). PIN2 protein levels remain low in G1 and S-phase and increase dramatically during G2 and M phase (Shen *et al.,* 1997; Kishi *et al.,* 2001). Overexpression of exogenous PIN2 showed that the levels remained consistent with the endogenous PIN2 levels, indicating that the regulation of PIN2 is post-translational rather than transcriptional (Shen *et al.,* 1997; Kishi *et al.,* 2001). However, protein levels of TRF1 have been shown to be consistent throughout the cell cycle (Zhong *et al.,* 1992; Wu *et al.,* 2008). More recent studies show that there may be a few exceptional distinctions in TRF1 and PIN2 function through their post-translational modifications. One notable study shows that Aurora A phosphorylation of S296, a residue unique to TRF1, contributes to the Aurora A overexpression mutant phenotype which results in centrosomal amplification and multinucleation during mitosis (Ohishi *et al.,* 2010). Also a preliminary *in vitro* CDK1 kinase assay on TRF1 and PIN2 revealed that the phosphorylation level of TRF1 is much higher than the phosphorylation level of PIN2 (fig.3.5A, lanes 2 and 3). In order to follow up on this preliminary experiment, we will use a well characterized CDK1 phosphorylation modification site, TRF1-T371, as a

starting point in identifying the potential differences that may be found between PIN2 and TRF1.

Figure 1.1 Diagram of open and close states of a telomere end. **(A)** Mammalian telomeric DNA with a 3' G rich overhang. **(B)** T-loop higher order structure, where the 3' G-rich overhang loops backwards and invades into a double stranded telomeric DNA. This process is believed to be assisted and maintained by the shelterin complex. TRF1/TRF2 = green, POT1/TPP1 = red, and Tin2 = orange. **(C)** Schematic diagram of shelterin proteins. Illustrations were adapted from Palm *et al.*, 2008.

A

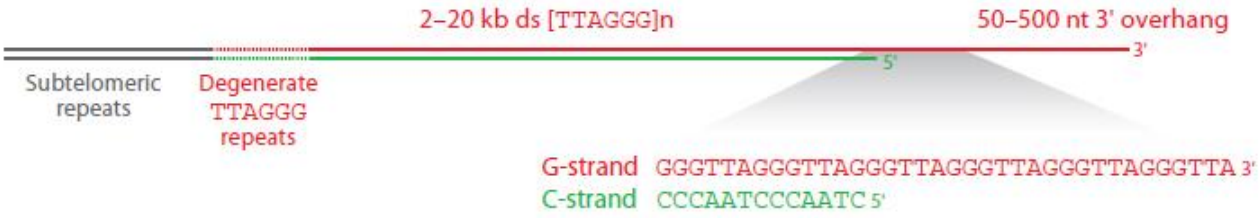
2–20 kb ds [TTAGGG]n
50–500 nt 3' overhang
3'
5'
Subtelomeric repeats
Degenerate TTAGGG repeats
G-strand GGGTTAGGGTTAGGGTTAGGGTTAGGGTTAGGGTTA 3'
C-strand CCCAATCCCAATC 5'

B

C

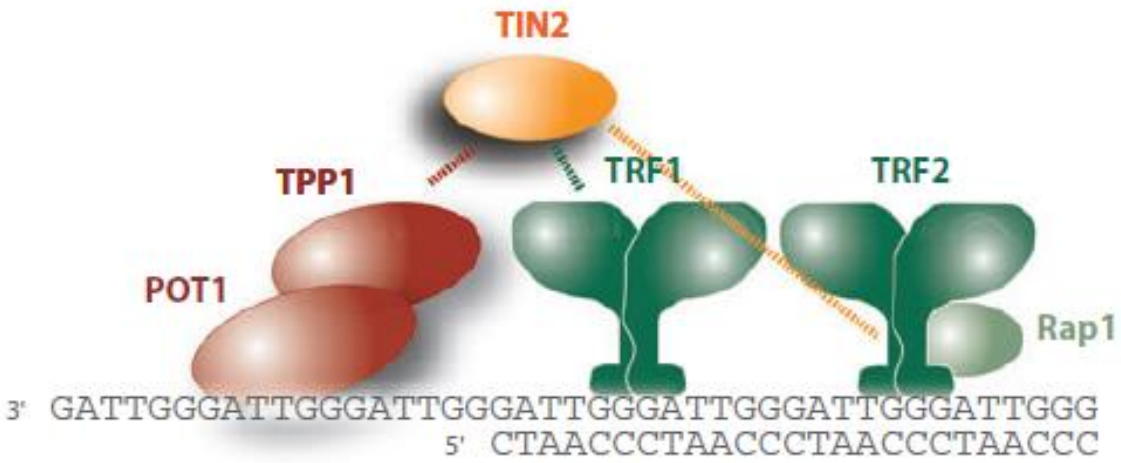
TIN2
TPP1
TRF1
TRF2
POT1
Rap1
3' GATTGGGATTGGGATTGGGATTGGGATTGGGATTGGGATTGGG
5' CTAACCCTAACCCTAACCCTAACCC

Figure 1.2 Schematic of TRF1. **(A)** Protein map of TRF1. **(B)** TRF1 blocks telomerase accessibility of telomeres in *cis* (Chang *et al.*, 2003). Linear line = telomeric DNA, square = non-telomeric DNA. **(C)** Documented TRF1 phosphorylation sites with respective identified kinase.

A


1
66
265
378
439
Acidic
TRFH
Linker
Myb

B

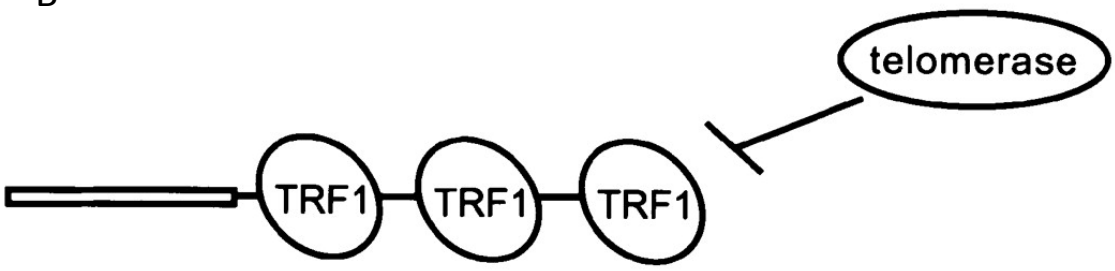
telomerase
TRF1
TRF1
TRF1

C

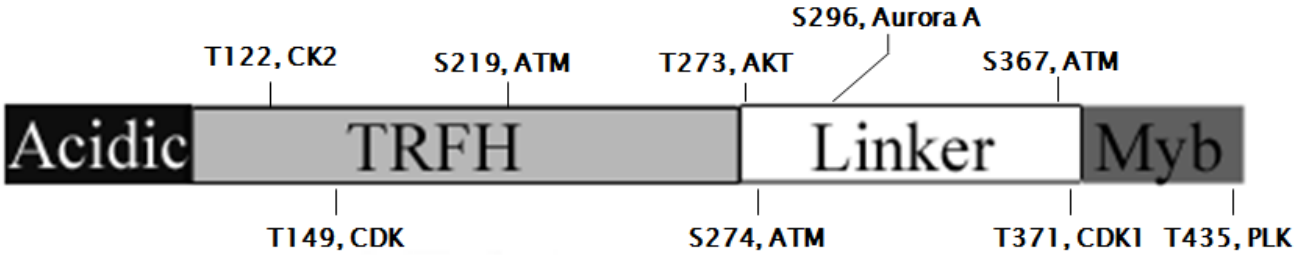

Table 1 Phosphorylation modification sites of TRF1

Site	Kinase	Description	Reference
T122	CK2	Involved in TRF1 binding to telomere DNA	Kim *et al.*, 2008
T149	CDK	Substrate binding for propyl isomerase, Pin1, allowing for TRF1 degradation during mitosis	Lee *et al.,* 2009
S219	ATM	Radiation sensitivity in AT cells and DNA damage response	Kishi *et al.,* 2001
T273	AKT	AKT overexpression results in telomere shortening	Wu *et al.,* 2009
S274	ATM	Decrease in telomere binding *in vitro*	Wu *et al.,* 2007
S296	Aurora A	TRF1 involved in kinetochore microtubule regulation	Ohishi *et al.,* 2009
S367	ATM	Dissociates from telomeres and forms protease inhibitor sensitive foci at S/G2 phase	Wu et *al.,* 2007; McKerlie *et al.,* 2012
T371	CDK1	Involved in sister telomere resolution	McKerlie and Zhu, 2011
T435	PLK	Increase telomere binding	Wu *et al.,* 2008

Figure 1.3 Protein map revealing the structural difference between TRF1 and PIN2.

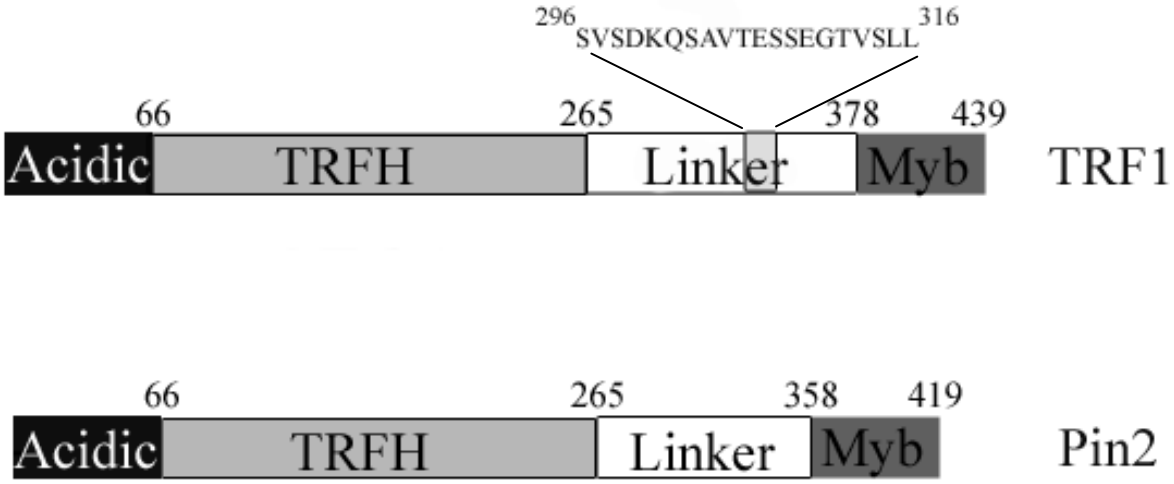
296
SVSDKQSAVTESSEGTVSLL
316
66
265
378
439
Acidic
TRFH
Linker
Myb
TRF1
66
265
358
419
Acidic
TRFH
Linker
Myb
Pin2

Chapter 2-Materials and Methods

2.1 Cloning of Plasmid Construct

Table 2.1 Oligo List

Oligo Number	Sequence
71	GCGC GAATTC TCA GTC TTC GCT GTC TGA GG
133	GTTTCAAAGAGTCAGCCGGT***GG***C***G***CCTGAAAAACATCGAGCT
134	AGCTCGATGTTTTTCAGG***C***G***CC***ACCGGCTGACTCTTTGAAAC
135	GTTTCAAAGAGTCAGCCGGT***GGA***TCCTGAAAAACATCGAGCT
136	AGCTCGATGTTTTTCAGGA***TCC***ACCGGCTGACTCTTTGAAAC
173	GCGC***AGATCT***TTTTCTTGTATCCAAATTAGCTTCAG
174	GCGC***AGATCT***CACAAGAATCTTTTCTTATCTAAG
175	GCGC***CTCGAG***GAATTCTCAGTCTTCGCTGTCTGAGGAAATCAG
372	GCGC**CTCGAG**TTATGAACATTCCCCATTCCAC

Table 2.2 Plasmid List

Construct	Plasmid Number	Name
pHis-TRF1SM	5043	Zhu Lab
pHis-TRF1SMT271A	5044	Zhu Lab
pHis-TRF1SMT271D	5045	Zhu Lab
pHis-TRF1SMS279A	5046	Zhu Lab
pHis-TRF1SMS279D	5047	Zhu Lab
pHis-TRF1SMT305A	5048	Zhu Lab
pHis-TRF1SMT305D	5049	Zhu Lab
pHis-TRF1SMT371A	5015	Zhu Lab
pHis-TRF1SMT371D	5074	Zhu Lab
pWZL-N-Myc-TRF1SM	3034	Zhu Lab
pWZL-N-Myc-TRF1SMT271A	5050	Zhu Lab
pWZL-N-Myc-TRF1SMT271D	5051	Zhu Lab
pRS	2041	Gift from Titia de Lange
pRS-shTRF1	3007	Zhu Lab
pLPC-N-Myc-TRF1SM(612-1320nt)	6034	Zhu Lab
pLPC-N-Myc-TRF1SM	6028	Zhu Lab
pLPC-N-Myc-TRF1SM(612-1320nt, 885nt BglII)	6029	Zhu Lab

pLPC-N-Myc-PIN2SM (612-1260nt)	6030	Zhu Lab
pLPC-N-Myc-PIN2SM-T351A (612-1260nt)	6031	Zhu Lab
pLPC-N-Myc-PIN2SM-T351D (612-1260nt)	6032	Zhu Lab
pHis-PIN2SM	6033	Zhu Lab
pHis-PIN2SM T351A	6034	Zhu Lab
pHis-PIN2SM T351D	6035	Zhu Lab

2.1.1 DNA Restriction Endonuclease Digestion

Restriction Digestion

One microlitre of mini-prep DNA was incubated with 0.5µl of restriction enzyme, 1µl of 10X Restriction enzyme buffer (respective to restriction enzyme, New England BioLabs Inc.), and 7.5µl of ddH_2O for 1 hour at 37°C. One microlitre of 10X loading dye was added to the digested samples and loaded onto a 1% agarose gel in 0.5X TAE (Tris, Acetic Acid, EDTA, EtBr) and ran for 1hr at 120 volts. The digested DNA bands were observed under an alpha imager.

2.1.2 Gel Purification

Two micrograms of mini-prep DNA (~5µl) was incubated with 1.25µl of restriction enzyme, 2.5µl of 10X restriction enzyme buffer, and the reaction volume was brought up to 25µl of ddH_2O for 2.5 hours at 37°C. The digested samples were loaded and ran on a 1% agarose gel in 0.5X TAE. The gel bands were excised and purified. The agarose gel band purification protocol and reagents used from illustra^{TM} GFX^{TM} PCR DNA and Gel Band Purification kit (GE Healthcare, lot#: 28-9034-70). The gel band of interest was excised using sterile razor blades and placed into a pre-weighed eppendorf tube. The tube

containing the excised band of interest was weighed once again and the weight of the excised gel piece was determined. Ten microlitres of Capture Buffer type 3 were added to every 10mg of excised agarose, inverted and left at 60°C until the agarose gel piece was fully dissolved. Once dissolved, the samples were spun down at 13,000RPM for 1 minute. The samples were then placed into a filter column (GFX Microspin^{TM} column, maximum amount ~500µl), incubated in the column for 1 minute, followed by a 1 minute 13,000RPM centrifugation. The flow through was discarded and 600µl Wash Buffer type 1 was added into the column, followed by immediate centrifugation at 13,000RPM for 1 minute. The column was then placed into an eppendorf tube, 25µl of 1XTE (10mM Tris-HCl [pH 8.0], 1mM EDTA [pH 8.0]) was added to the column for 1 minute, and the samples were spun at 13,000 RPM for 1 minute. The flow through was kept and a few microlitres of sample were run on an agarose gel to assess the quality and success of the purification.

2.1.3 DNA ligation protocol

Half a microlitre of vector DNA was incubated with 7.5µl of insert DNA, 1µl of 10X ligation buffer (New England BioLabs In(C) and 1µl of T4 DNA ligase (New England BioLabs Inc.) and placed at room temperature for two to three hours and then stored at -20°C.

2.1.4 Transformation of Plasmid DNA into TOP10 cells

Ligated DNA transformation

Five microlitres of ligated DNA was added to 100µl of TOP10 cells. The mixture (TOP10 cells and ligated DNA) was placed on ice for 30 minutes. The cells were heat shocked at 42°C for 45 seconds and then allowed to cool on ice for 2 minutes. Nine hundred microlitres of LB (0.5% Bacto™ yeast extract, 1% Bacto™ tryptone, 17.1 mM NaCl, and 2.8 mM NaOH) was added into the mixture tube and the cells recovered for 1 hour on a 37°C shaker (~ 200RPM). After the 1 hour incubation, the tube was spun at 13,000 RPM for 30 seconds. Nine hundred microlitres of the supernatant was removed and the remaining 100 µl mixture was vortexed to effectively resuspend the pellet. The resuspended pellet was plated on to an LB agar plate (0.5% Bacto™ yeast extract, 1% Bacto™ tryptone, 17.1 mM NaCl, and 2.8 mM NaOH, 1.5% agar, 100µg/ml of ampicillin). Another 100 µl of LB was added to the mixture tube and then plated to a second LB agar plate referred to as the 'wash plate.' The plate was placed at 37°C for 12-16 hours and then stored at 4°C.

Plasmid DNA transformation

Add 1µl of ligated DNA reaction into 30µl of TOP10 cells. The mixture (TOP10 cells and ligated DN(A) was placed on ice for 15 minutes. The cells were heat shocked at 42°C for 45 seconds and then allowed to cool on ice for 2 minutes. Nine hundred microlitres of LB was added into the mixture tube and the cells recovered for 1 hr on a 37°C shaker

(~200RPM). After the 1 hr incubation, 50µl of the 1ml transformation tube was plated on a LB agar plate. The plate was placed at 37°C for 12-16 hours and then stored at 4°C.

2.1.5 Minipreparation of plasmid DNA

A single colony from a transformed LB agar plate is picked and inoculated into 2ml of LB containing 100µg/ml of ampicillin in an 8ml inoculation tube. The inoculants were placed in a 37°C shaker for 12-16 hours. Overnight cultures were transferred into eppendorf tubes and collected by centrifugation at 13,000 RPM for 1 minute. The supernatant was removed and the bacterial pellet was resuspended in 100µl of mini-prep solution 1 (50mM glucose, 25mM Tris-HCl [pH 8.0], 10mM EDTA [pH8.0]). Two hundred microlitres of freshly made mini-prep solution 2 (200mM NaOH, 1% SDS) was added to the resuspended bacteria, and the tube was inverted and stored on ice for 3-4 minutes to lyse the resuspended bacteria. One hundred and fifty microlitres of mini-prep solution 3 (3M potassium acetate [pH 5.0]) was added to the lysates, inverted and stored on ice for 3-5 minutes to neutralize the effects of the solution 2 buffer. The samples were spun at 13,000RPM in 4°C for 5 minutes. After the 5 minute centrifugation, the supernatants were collected and an equal volume of phenol chloroform was added, and the phenol/supernatant mixtures were vortexed and spun at 13,000RPM for 2 minutes at 4°C. The upper aqueous layer was collected and transferred to a fresh tube, 800µl of 95% ethanol was added and this was vortexed and spun at 13,000RPM for 5 minutes at 4°C. The 95% ethanol was discarded and the DNA pellet was washed twice with 70% ethanol. Once the DNA pellet was air dried, the pellets were resuspended in 30-40µl of 1XTE

buffer (10mM Tris-HCl [pH 8.0], 1mM EDTA [pH 8.0], 20µg/ml of RNase (A). The DNA samples were then stored at -20°C.

2.1.7 Generation of pHis-Parallel 2-PIN2SM and PIN2 mutants

pHis-Parallel 2-PIN2SM

First Step: pLPC-N-Myc vector (black circle) was digested with EcoRI, followed by alkali phosphatase treatment (Fig.2A, Step 1). The linearized vector was ligated with a 700 bp insert containing TRF1 fragment 615-1320nt. The 700 bp insert was isolated from an EcoRI digestion of pWZL-N-Myc TRF1SM (red circle) (Fig.2A, Step 1). Both the isolated vector and insert were ligated together to produce pLPC-N-Myc-TRF1SM (612-1320nt) (Fig.2A, Step 1).

Second Step: pLPC-N-Myc-TRF1SM (612-1320nt) was double digested with BamHI and BglII. A large fragment about 6 kb in size was purified as a vector. The isolated vector was ligated with a 300bp insert (represented by a green line) containing the first of two fragments required to produce the 60 nucleotide deletion found in the PIN2 cDNA (Fig.2A, Step 2). The insert was generated through PCR, followed by BamHI and BglII double digestion. The PCR was carried out by using oligos 372/173 as primers and pWZL-N-Myc-TRF1SM (red circle) as a template (Fig.2A, Step 2). The ligated vector and insert gave rise to pLPC-N-Myc-TRF1SM (885nt BglII 612-1320nt). Positive clones were screened with BamHI and BglII double digestion.

Third Step: pLPC-N-Myc-TRF1SM (885nt BglII, 612-1320nt) was digested with BglII and treated with alkali phosphatase (Fig.2B, step 3). The linearized vector was ligated with a 200 bp insert (blue line) to generate pLPC-N-Myc-PIN2SM(612-1260nt) (Fig.2B, step 3). The insert was generated through PCR, which was then digested with BglII. The PCR was carried out by using oligos 174/175 as primers and pHis-Parallel 2- TRF1SM (orange circle) as a template (Fig.2B, step 3). The 200 bp insert is the second and final fragment required to generate the 60 nucleotide deletion found in the PIN2 cDNA. The construct was screened with BglII digestion to verify the presence of the 200 bp insert (blue line) and PCR screening was used with both oligos 372/134 and 372/136 to verify orientation of the insert fragment.

Fourth Step: pHis-Parallel 2-TRF1SM (orange circle) was digested with EcoRI and treated with alkali phosphatase (Fig.2B, step 4). A large fragment of about 5.5 kb was purified as vector. pLPC-N-Myc-PIN2SM (612-1260nt) insert was purified through EcoRI digestion followed by gel purification (Fig.2B). The purified insert (green/blue/red fragment) and vector (orange fragment) were ligated together to generate pHis-Parallel 2-PIN2SM (Fig.2B). The newly formed constructs were screened through EcoRI digestion, BglII digestion, and verified through DNA sequencing analysis.

pHis-Parallel 2-PIN2SM-T351A

First and Second step: please refer to cloning strategy for pHis-Parallel 2 –PIN2SM (Fig.2A).

Third Step: pLPC-N-Myc-TRF1SM (885nt BglII, 612-1320nt) was digested with BglII and treated with alkali phosphatase (Fig.2C, step 3). The linearized vector was ligated with a 200 bp insert (purple line) to generate pLPC-N-Myc-PIN2SM T351A (612-1260nt) (Fig.2C, step 3). The 200 bp insert is the second and final fragment required to generate the 60 nucleotide deletion found in the PIN2 cDNA. The insert also contains the T351A mutation site. The insert was generated through PCR, which was then digested with BglII. The PCR was carried out by using oligos 174/175 as primers and pHis-Parallel 2- TRF1SM T371A (grey circle) as a template (Fig.2C, step 3). The construct was screened with BglII digestion to verify the presence of the 200 bp insert and PCR screening was used with oligo 71/133 to verify orientation of the insert fragment.

Fourth Step: pHis-Parallel 2-TRF1SM (orange circle) was digested with EcoRI and treated with alkali phosphatase (Fig.2C, step 4). A large fragment of about 5.5 kb was purified as vector. pLPC-N-Myc-PIN2SM-T351A (612-1260nt) insert was purified through EcoRI digestion followed by gel purification (Fig.2C, step 4). The purified insert (green/purple/red fragment) and vector (orange fragment) were ligated together to generate pHis-Parallel 2-PIN2SM-T351A (Fig.2C, step 4). The newly formed construct was screened through EcoRI digestion, BglII digestion, NarI digestion and verified through DNA sequencing analysis.

pHis-Parallel 2-PIN2SM-T351D

First step and Second step: please refer to cloning strategy for pHis-Parallel 2 –PIN2SM (Fig.2A).

Third Step: pLPC-N-Myc-TRF1SM (885nt BglII, 612-1320nt) was digested with BglII and treated with alkali phosphatase (Fig.2C, step 3). The linearized vector was ligated with a 200 bp insert (purple line) to generate pLPC-N-Myc-PIN2SM T351D (612-1260nt) (Fig.2C, step 3). The 200 bp insert is the second and final fragment required to generate the 60 nucleotide deletion found in the PIN2 cDNA. The insert also contains the T351D mutation site. The insert was generated through PCR, which was then digested with BglII. The PCR was conducted out by using oligos 174/175 as primers and pHis-Parallel 2- TRF1SM T371D (grey circle) as a template (Fig.2C, step 3). The construct was screened with BglII digestion to verify the presence of the 200 bp insert (purple fragment) and PCR screening was used with oligos 71/135 to verify orientation of the insert fragment.

Fourth Step: pHis-Parallel 2-TRF1SM (orange circle) was digested with EcoRI and treated with alkali phosphatase (Fig.2C, step 4). A large fragment of about 5.5 kb was purified as vector. pLPC-N-Myc-PIN2SM-T351D (612-1260nt) insert was purified through EcoRI digestion followed by gel purification (Fig.2C, step 4). The purified insert (green/purple/red fragment) and vector (orange fragment) were ligated together to create pHis-Parallel 2-PIN2SM-T351D (Fig.2C, step 4). The construct was screened through EcoRI digestion, BglII digestion, BamHI digestion and verified through DNA sequencing analysis.

2.2 Protein Analysis

2.2.1 Bradford Assay

Protein concentrations were determined through a Bradford assay. One microlitre of protein extract was added to 199µl of water and 800µl of Bradford solution (25% Bio-Rad Bradford solution and 75% water). The mixture was vortexed and left to incubate at room temperature for 15 minutes. The blank control consisted of 200µl water and 800µl Bradford solution. After 15 minutes, readings were taken of the Bradford samples using a spectrophotometer (Beckman Coulter, DU®530) at OD_{595}. Protein concentrations were determined through calculating absorbency values in a standard formula derived from a BSA curve.

2.2.2 Recombinant protein harvest from BL21 pLysS

Day 1: Transformation into BL21 *pLysS* (*E.coli* strain)

Please refer to 'transformation protocol of mini-prep DNA'. BL21 pLysS *E. coli* strain was used instead of the TOP10 cells.

Day 2: Inoculation of starter culture

Please refer to the inoculation protocol in the "Cloning of plasmid construct" section. Five millilitres of LB was used instead of 2ml from the inoculation protocol.

Day 3: Induction of recombinant protein

The starter culture was added to 500ml of LB (100µg/ml of ampicillin) in a 1:100 dilution. The flask was grown to OD_{600} of 0.5 in a 37°C shaker (200RPM). The flask was induced with IPTG (1mM) overnight in a room temperature shaker (200RPM).

Day 4: Protein harvest

The induced culture was transferred into a 420ml centrifuge bottle and spun down at 4000 RPM for 10 minutes. The pellet was washed with chilled 1XPBS buffer (pH 7.4) and spun down at 4000 RPM for 10 minutes at 4°C. The washed pellet was resuspended in 1X Binding buffer (0.5M NaCl, 20mM Tris-HCl [pH 7.9], 1mM of PMSF) and sonicated (20 second pulse setting, 20 second rest, 50% output control, 5 duty cycle) five to six times on ice. The lysates were spun down at 13,000 RPM for 15 minutes at 4°C. The soluble fraction was collected and incubated with charged nickel resin beads (1ml 50% slurry, Qiagen) for 1.5 hours at 4°C. The beads were washed with 3 bed volumes of 1X binding buffer at 4000 RPM for 10 minutes at 4°C. The second and third washes were completed with 3 bed volumes of 1Xwash buffer (60mM imidazole, 1mM PMSF) at 4000 RPM for 10 minutes at 4°C. The samples were eluted with 2 bed volumes of 1X elution buffer (1M imidazole, 0.5M NaCl, 20mM Tris-HCl [pH 7.9]). After three elutions, the eluted samples were dialyzed in KCl Dialysis buffer (500mM KCl, 20mM Hepes [pH 7.9], 20% glycerol, 3mM $MgCl_2$, 1mM DTT, and 1mM PMSF) for 16 hours at 4°C. After dialysis, Bradford readings were taken to determine protein concentrations of the eluted samples. The recombinant proteins were aliquoted and stored at -80°C.

Recombinant proteins were loaded on a SDS-PAGE gel (6% stacking and 8% separating) to determine protein quality. The protein gel was visualized through Coomassie staining (30% methanol, 10% acetic acid, 0.1% Coomassie Blue 250) for 15 minutes at room temperature and left destaining (8% acetic acid, and 20% methanol) overnight at room temperature.

2.3 Radioactive Analysis

2.3.1 EMSA

Gel shift Condition 1

Bacteria-derived recombinant protein (60ng, 120ng, 240ng, 360ng) was mixed in a 20µl reaction consisting of 10µl 2x GS buffer (20mM HEPES-KOH [pH 7.9], 150mM KCl, 4% (w/v) Ficoll, 5%(w/v) glycerol, 1mM EDTA, 0.1mM $MgCl_2$, 0.5mM DTT), 0.5µg of sheared *E. coli* genomic DNA, 50ng of β-casein and 0.5µl of pTH12 end labeled probe at room temperature for 20 minutes. The reactions were loaded onto a 0.7% agarose gel and ran in 0.1XTBE (8.9mM Tris, 8.9mM boric acid and 0.2mM EDTA [pH8.0]) at 130V for 1 hour at room temperature. The gel was dried on a slab gel dryer (SGD2000, Thermo Scientific) for 2.5 hours at 80°C and exposed in a PhosphoImager screen cassette (Amersham Biosciences) overnight. The exposed screen was scanned into a PhosphoImager scanner (Storm 820, Amersham Pharmacia Biotech). The data observed was quantified in ImageQuant software v5.2.

Gel Shift Condition 2

The protocol is similar to gel shift condition 1, with exception of the addition 2µg of sheared *E. coli* genomic DNA and 70µg of BSA in the gel shift binding reaction.

2.3.2 Radioactive kinase assay

One microgram of recombinant protein was incubated for 30 minutes at 30°C in a 15µl reaction with 1x NEBuffer for Protein Kinases (PK, NEB, P6020), 10 units or 10units of recombinant CDK1-cyclin B (NEB, P6020), and 50µCi of γ-^{32}P-ATP. The kinase reaction was run on SDS-PAGE gel electrophoresis, Coomassie stained, and destained. The destained gel was dried on a slab gel dryer for 2 hours at 70°C and exposed on a phosphoimager cassette. The data collected was observed on ImageQuant.

Figure 2 PIN2 cloning strategy. **(A)** Schematic diagram of the first two steps of PIN2 and PIN2 mutant cloning. **(B)** Schematic diagram for steps three and four of pHis-Parallel 2-PIN2SM cloning. **(C)** Schematic diagram for steps three and four of pHis-Parallel 2-PIN2SM-T351A and pHis-Parallel 2- PIN2SM-T351D cloning.

A

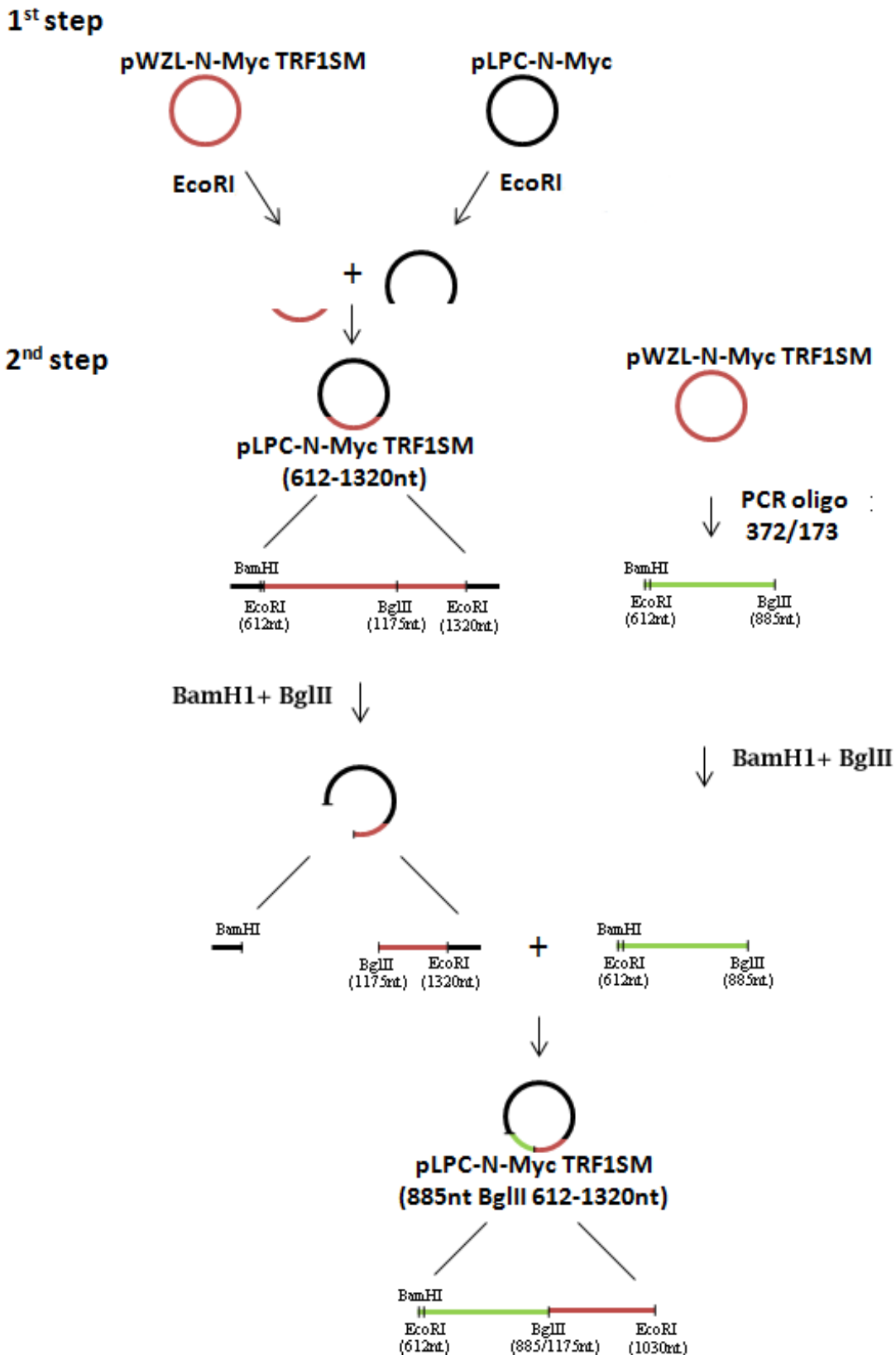
1st step
pWZL-N-Myc TRF1SM
pLPC-N-Myc
EcoRI
EcoRI
+
2nd step
pLPC-N-Myc TRF1SM
(612-1320nt)
BamHI
EcoRI
(612nt)
BglII
(1175nt)
EcoRI
(1320nt)
pWZL-N-Myc TRF1SM
PCR oligo
372/173
BamHI
EcoRI
(612nt)
BglII
(885nt)
BamH1+ BglII
BamH1+ BglII
BamHI
BglII
(1175nt)
EcoRI
(1320nt)
+
BamHI
EcoRI
(612nt)
BglII
(885nt)
pLPC-N-Myc TRF1SM
(885nt BglII 612-1320nt)
BamHI
EcoRI
(612nt)
BglII
(885/1175nt)
EcoRI
(1030nt)

B

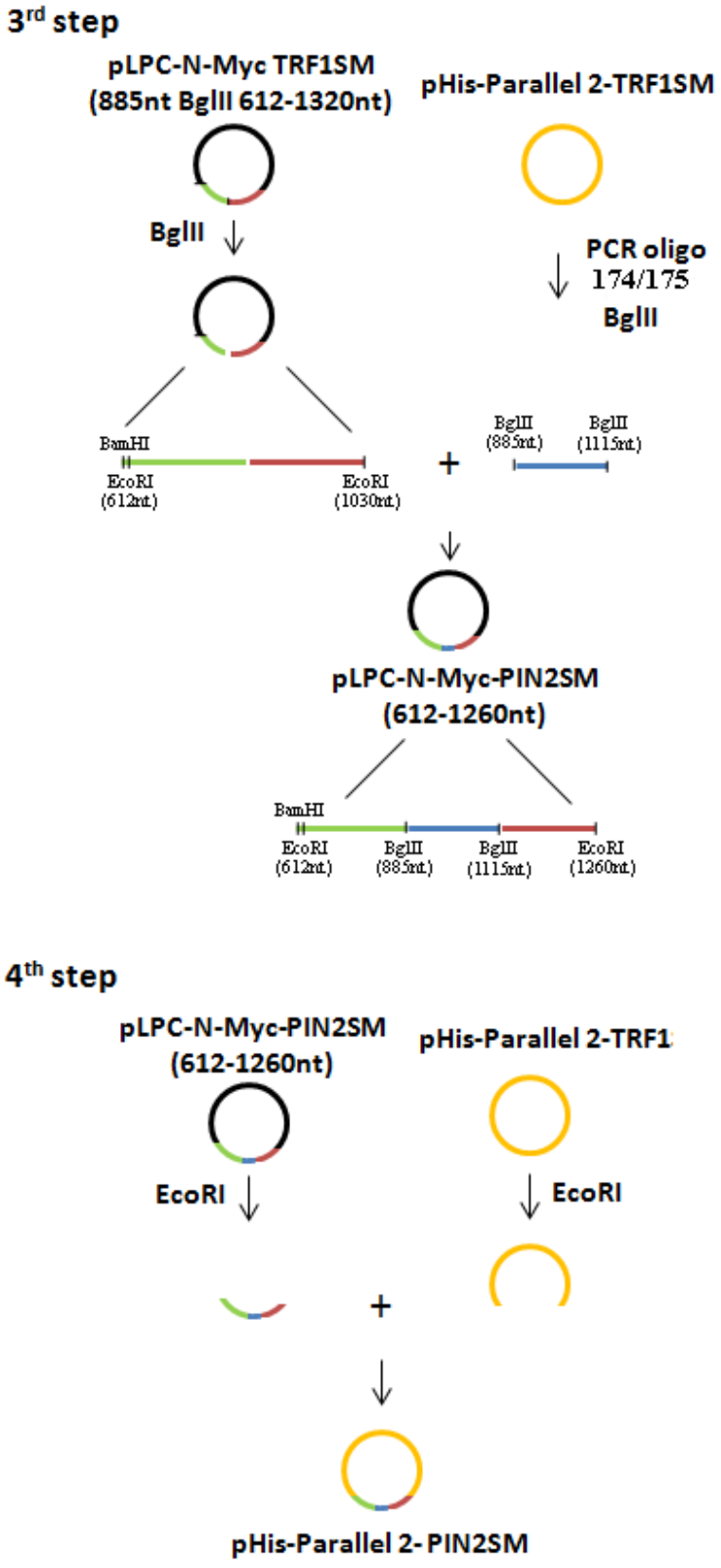
3rd step
pLPC-N-Myc TRF1SM
(885nt BglII 612-1320nt)
pHis-Parallel 2-TRF1SM
BglII
PCR oligo
174/175
BglII
BamHI
EcoRI
(612nt)
EcoRI
(1030nt)
BglII
(885nt)
BglII
(1115nt)
pLPC-N-Myc-PIN2SM
(612-1260nt)
BamHI
EcoRI
(612nt)
BglII
(885nt)
BglII
(1115nt)
EcoRI
(1260nt)
4th step
pLPC-N-Myc-PIN2SM
(612-1260nt)
pHis-Parallel 2-TRF1
EcoRI
EcoRI
pHis-Parallel 2- PIN2SM

C

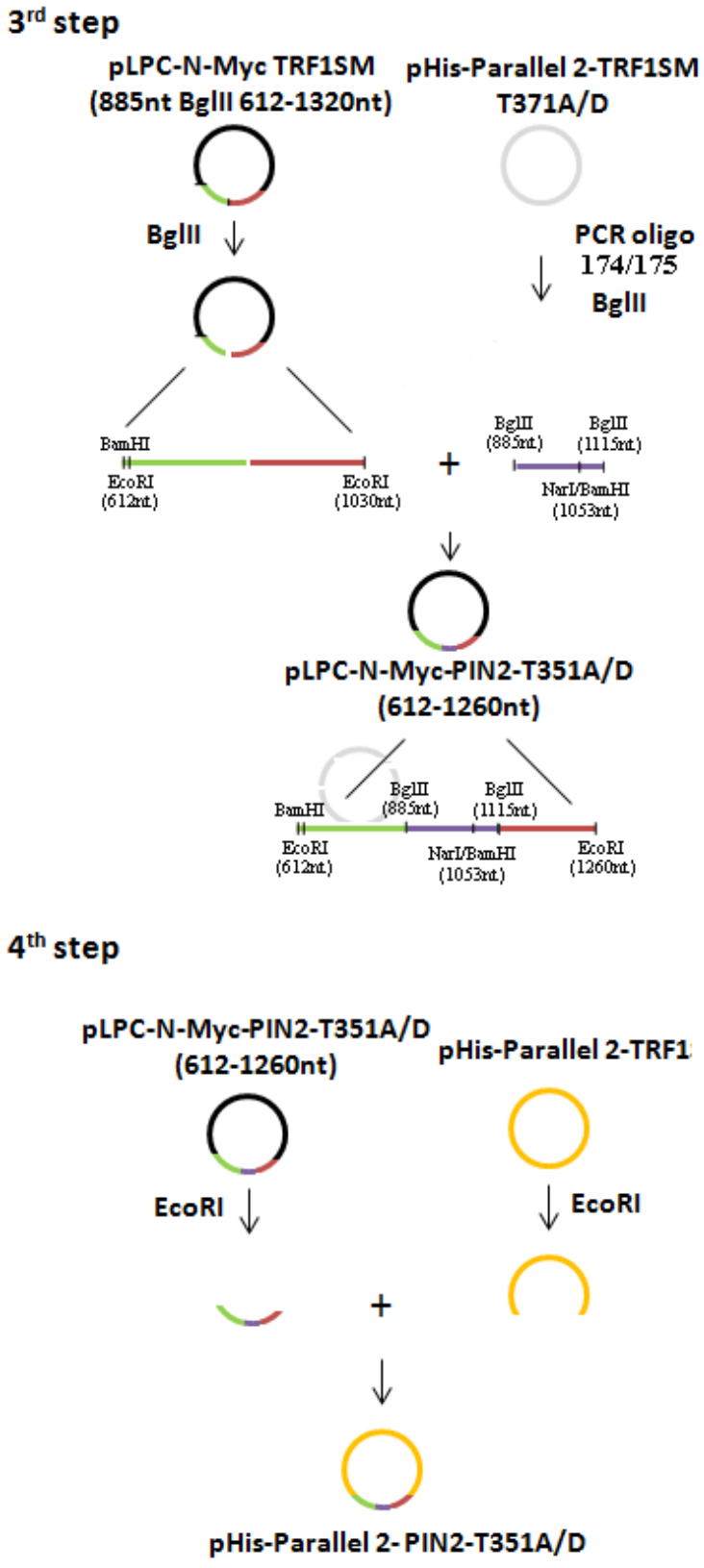
3rd step
pLPC-N-Myc TRF1SM
(885nt BglII 612-1320nt)
pHis-Parallel 2-TRF1SM
T371A/D
BglII
PCR oligo
174/175
BglII
BamHI
EcoRI
(612nt)
EcoRI
(1030nt)
+
BglII
(885nt)
BglII
(1115nt)
NarI/BamHI
(1053nt)
pLPC-N-Myc-PIN2-T351A/D
(612-1260nt)
BamHI
EcoRI
(612nt)
BglII
(885nt)
BglII
(1115nt)
NarI/BamHI
(1053nt)
EcoRI
(1260nt)
4th step
pLPC-N-Myc-PIN2-T351A/D
(612-1260nt)
pHis-Parallel 2-TRF1
EcoRI
EcoRI
+
pHis-Parallel 2- PIN2-T351A/D

Chapter 3 – Results

Characterization of TRF1 phosphorylation sites T271, S279 and T305

3.1 Generation of Recombinant pHis-Parallel 2-PIN2SM and PIN2SM mutant plasmid constructs

pHis-Parallel 2-PINSM, pHis-Parallel 2-PIN2SM T351A, and pHis-Parallel 2-PIN2SM T351D were all generated in four steps (Fig.2A-C). The vectors created in the first two steps were used in generating all three PIN2 constructs (Fig.2A). In the first step, EcoRI digestion was used to isolate TRF1SM (612-1320nt) insert fragment, which was then ligated into a pLPC-N-Myc vector (black circle) to generate plpc-n-myc-TRF1SM (612-1320nt) (Fig.2A, step 1). The newly generated vector was verified through EcoRI digestion yielding the expected 708 bp insert (red fragment; Fig.3.1A). The pLPC-N-Myc construct was used as a vector backbone due to the absence of the BglII restriction site which is necessary for PIN2 cloning steps 2 and 3.

In Step 2, the construct pLPC-N-Myc-TRF1SM (885nt BglII, 612-1320nt) was generated and screened through BamHI and BglII double digestion verifying the presence of the 295 bp insert (green fragment; Fig.3.1B). Two potential positive clones 9 and 12 were identified (Fig.3.1B). The 295 bp insert is the first of two PCR fragments required

to produce the 60 nucleotide deletion found in the PIN2 cDNA (green fragment; Fig.2A, Step 2).

In step 3, the pLPC-N-Myc-PIN2SM (612-1260nt), pLPC-N-Myc-PIN2SM T351A (612-1260nt), and pLPC-N-Myc-PIN2SM T351D (612-1260nt) constructs were generated. The constructs were verified in two steps. The first verification step was a BglII digestion which was used to assess the presence of the 230 bp insert (blue fragment for PIN2SM and purple fragment for PIN2SM T351A/D) which contains the second and final PCR fragment required to generate the 60 nucleotide deletion found in PIN2 cDNA (Fig.2B,C; Fig.3.1C1). The 230 bp insert (purple fragment) also contains the T351A/D mutations for constructs pLPC-N-Myc-PIN2SM T351A (612-1260nt), and pLPC-N-Myc-PIN2SM T351D (612-1260nt) respectively (Fig.3.1C3). The second verification step involves using PCR screening to determine the orientation of the 230 bp insert. PCR screening of pLPC-N-Myc-PIN2SM (612-1260nt) clones were verified with two sets of primers 372/134 and 372/136 which produced a 438 bp product (Fig.3.1C2). pLPC-N-Myc-PIN2SM (612-1260nt) clone 14 was identified as a positive clone (Fig.3.1C1-2). PCR screening of pLPC-N-Myc-PIN2SM T351A/D (612-1260nt) were verified with primers 133/71 and 135/71, respectively, which produced a 207 bp product (Fig.3.1C3). pLPC-N-Myc-PIN2SM T351A (612-1260nt) clone 18 and pLPC-N-Myc-PIN2SM T351D (612-1260nt) clone 15 were identified as positive clones (Fig.3.1C1-3).

In step 4, one verification step was required to determine the authenticity of pHis-Parallel 2-PIN2SM construct (Fig.3.1D1). BglII digestion screen was used to validate the

presence of the insert fragment 612-1260nt (green/blue/red) of the PIN2SM construct and its orientation (Fig.3.1D1-3). The BglII digestion of pHis-Parallel 2-PIN2SM results in a 230 bp (blue) and an 885 bp (orange/green) insert fragment. The 230bp fragment (blue) indicates the presence of the 60 nucleotide deletion found in PIN2 cDNA. The 885bp (orange/green) fragment reveals the correct orientation of the EcoRI fragment (green/blue/red fragment; Fig.3.1D1). If the EcoRI fragment was ligated in the wrong orientation, a BglII digestion would result in a 700bp fragment instead (Fig.3.1D1, Clone 10). pHis-Parallel 2-PIN2SM clone 11 was confirmed positive (Fig.3.1D1).

In contrast, two verification steps were used to determine the authenticity of pHis-Parallel 2-PIN2SM T351A, and pHis-Parallel 2-PIN2SM T351D (Fig.3.1D). The BglII digestion of pHis-Parallel 2-PIN2SM T351A/D results in a 230 bp (purple) and an 885bp (orange/green) insert fragment. The 230 bp fragment (purple) indicates the presence of the 60 nucleotide deletion found in PIN2 cDNA. The 885 bp fragment (orange/green) reveals the correct orientation of the EcoRI fragment (green/purple/red) (Fig.3.1D2-3). If the EcoRI fragment (green/purple/red) was ligated in the wrong orientation, a BglII digestion would result in a 700 bp fragment instead (Fig.3.1D1, Clone 10). It is important to note that the 230 bp fragment (purple) of pHis-Parallel 2 –PIN2SM T351A was not shown (Fig.3.1D3). However, the presence of the 230 bp BglII fragment (purple) was confirmed through DNA sequencing. For the second confirmation step, NarI and BamHI digestions were conducted to verify the presence of the T351A and T351D mutation sites respectively (Fig.3.1D3). NarI digestion of a positive clone of pHis-Parallel 2-PIN2SM T351A would produce a 1182 bp (orange), a 4150 bp

(purple/red/orange), and a 1060 bp (orange/green/purple) fragment (Fig.3.1D3). A negative NarI digestion clone would only yield a 1182 bp and a 5210 bp fragment (Fig 3.1D3; pHis-Parallel 2-PIN2SM clone 11). pHis-Parallel 2-PIN2SM T351A clone 10 was identified as a positive clone (Fig.3.1D3). BamHI digestion of pHis-Parallel 2-PIN2SM T351D positive clone would produce an insert fragment of 1053 bp (orange/green/purple) in length, whereas a pHis-parallel-2 PIN2SM construct lacking the T351D site would only produce a linear vector (Fig.3.1D3; pHis-Parallel 2-PIN2SM clone 11). pHis-Parallel 2-PIN2SM T351D clone 8 was identified as a positive clone (Fig.3.1D3). All PIN2 positive clones were finalized through DNA sequencing.

3.2 Recombinant protein expression and purification of TRF1 and PIN2 mutants

To analyze TRF1 phosphorylation *in vitro*, alanine (phosphorylation dead) and aspartic acid (phosphomimic) TRF1 recombinant mutants were generated for phosphorylation sites, T271, S279 and T305 (Fig. 3.2A). The three potential TRF1 phosphorylation sites are all found in the linker region (Fig. 3.2A). Interestingly, T305A/D is found in the TRF1 exclusive 20aa section of the linker region that is absent in PIN2 (Shen *et al.*, 1997; Fig. 3.2A). His-TRF1-T371A/D mutants were selected to compare any potential functional differences to its PIN2 counterpart, His-PIN2 T351A/D (Fig. 3.2A). The PIN2 mutants were generated in a similar manner to the other phosphorylation mutant constructs.

The recombinant proteins were expressed and purified by nickel bead batch purification. TRF1 and PIN2 mutant protein concentrations were taken through Bradford readings. Protein quality and relative concentrations were assessed through SDS-PAGE assay and visualized through Coomassie staining (Fig. 3.2B). The recombinant TRF1 proteins run at about 65kDa, whereas the PIN2 proteins run slightly faster, at about 60kDa. Although there are some degradation products, the full length form attributes to the vast majority of band intensity visualized through Coomassie staining (~ at least 80%) (Fig. 3.2B).

3.3 Mutation analysis of TRF1 phosphorylation sites T271, S279 and T305

3.3.1 TRF1 mutants show no binding defects under gel shift condition 1

It has previously been shown that phosphorylation at the linker region can regulate TRF1 association with telomeric DNA (Wu *et al.*, 2007; Wu *et al.*, 2009; McKerlie, 2011; McKerlie *et al.*, 2012). To determine whether any putative T271, S279 or T305 sites may be involved in DNA binding, *in vitro* gel shift assays were conducted on the recombinant aspartic acid and alanine mutants of TRF1-T271, TRF1-S279, and TRF1-T305. Gel shift assays for all TRF1 mutants do not show any drastic differences in binding as compared to wild type (Fig. 3.3A). The quantification analysis confirms that there is no statistically significant difference between the three TRF1 mutants and wild type TRF1 under gel shift condition 1 (0.5ug of sheared *E. coli* DNA) (Fig.3.3B-D) (*Wu et al.*, 2007). It has been shown that certain TRF1 mutants only exhibit telomere binding

defects under gel shift condition 2 (2ug of sheared *E. coli* DNA), such as TRF1-S367D (McKerlie *et al.,* 2012).

3.3.2 TRF1 mutant T271D displays DNA binding defect under gel shift condition 2

Gel shift assays conducted under condition 2 contains 2µg of sheared *E. coli* DNA and 70µg of BSA (McKerlie *et al.,* 2012). The addition of more competitor DNA is designed to reduce the number of non-specific protein-probe DNA interaction that may obscure any potential binding defects (reviewed by Hellman *et al.,* 2007). Gel shift assays conducted on TRF1-S279 and T305 mutants reveal no binding defects under gel shift condition 2 (Fig. 3.4 A-D).

In contrast, His-TRF1-T271D displays a binding defect under gel shift condition 2 (Fig. 3.4 E). As wild type TRF1 and TRF1-T271A begin to saturate at 480ng, TRF1-T271D binds to telomeric DNA at around ~60% efficiency (Fig. 3.4 F). These data may suggest that TRF1 phosphorylation at T271 may negatively regulate telomeric DNA binding.

3.4 *In vitro* characterization of TRF1 and PIN2 mutant constructs

In vitro analysis of CDK1 kinase assay revealed that CDK1 phosphorylation levels between TRF1 and PIN2 were significantly different (Fig.3.5A). It has recently been documented that TRF1-T371 site is phosphorylated by CDK1 during mitosis (McKerlie, 2011). This phosphorylation site is also found in the TRF1 isoform, PIN2. It was of great interest to determine whether the PIN2 isoform would be modified by CDK1

at the same site as TRF1 and whether the modification at this site in PIN2 would affect binding as it does in TRF1.

3.4.1 PIN2 is phosphorylated at site T351 by CDK1 via *in vitro* kinase assays, but the net level of PIN2 phosphorylation is significantly lower than TRF1

Consistent with previous data, the substitution of an alanine mutation at TRF1-T371 abrogates net TRF1 phosphorylation by CDK1 (McKerlie, 2011; Fig.3.5A). There also appears to be a slight reduction in net PIN2 phosphorylation by CDK1, when an alanine mutation is introduced at site T351 (Fig.3.5A). This data suggests that both T371 and T351 of TRF1 and PIN2 respectively are targets of CDK1. Interestingly, the net phosphorylation of PIN2 is significantly lower than the net phosphorylation of TRF1 by CDK1. This may suggest that TRF1 has additional CDK1 target sites which may not be recognized on PIN2 or that TRF1 is simply a better target substrate for CDK1.

3.4.2 Phosphomimic mutation of T351 of PIN2 does not abrogate telomere binding

It has previously been reported that a phosphomimic substitution at T371 of TRF1 results in failure of TRF1 to associate with telomeric DNA (McKerlie, 2011; Fig. 3.5D, E). To determine whether a phosphomimic substitution at T351 of PIN2 would affect DNA binding, a gel shift condition 1 assay was performed. Interestingly, the *in vitro* gel shift assay of PIN2 and PIN2 T351 mutants did not exhibit any binding defects that were comparable to TRF1 and TRF1-T371 mutants (Fig. 3.5B-E). It is important to note however, that both PIN2 mutants bound slightly weaker to DNA in comparison to wild

type PIN2 but were comparable to the DNA binding efficiency observed with wild type TRF1(Fig.3.5C).

Figure 3.1 pHis-Parallel 2-PIN2SM, pHis-Parallel 2-PIN2SM T351A, pHis-Parallel 2-PIN2SM T351D cloning in four steps. (A) Step 1, Schematic diagram of pLPC-N-Myc-TRF1SM (612-1320nt) and EcoRI digestion screen verifying the presence of the 708 bp insert (red fragment). **(B)** Step 2, BamHI and BglII double digestion screen on pLPC-N-Myc-TRF1SM (885nt BglII, 612-1320nt) confirming the presence of the first PCR insert (green fragment) required in creating the 60 nucleotide deletion. A schematic diagram is provided to help visualize the BamHI and BglII double digestion of a pLPC-N-Myc-TRF1SM (885nt BglII, 612-1320nt) positive clone. **(C)** Step 3, BglII digestion screen **(C1)** and PCR orientation screen **(C2-3)** on pLPC-N-Myc-PIN2SM (612-1260nt), and pLPC-N-Myc-PIN2SM T351A/D (612-1260nt) constructs. Schematic diagrams to visualize each verification step have been included for each respective gel picture. **(D)** Step 4, verification of pHis-parallel 2-PIN2SM, and pHis-Parallel 2-PIN2SM T351A/D. **(D1-3)** BglII digestion screen was used to verify the orientation of the EcoRI PIN2SM (green/blue/red) and PIN2SM T351 mutant (green/purple/red) inserts. **(D3)** NarI and BamHI digestion screen was used to verify the PIN2T351A and T351D mutation sites respectively. NarI and BamHI digestion of pHis-Parallel 2- PIN2SM was used as a negative control. White asterisks represent single bands that may appear smeary. Schematic diagrams are provided to help visualize verification steps. Black asterisks represent the predicted band of interest. N.S = not seen on gel.

A

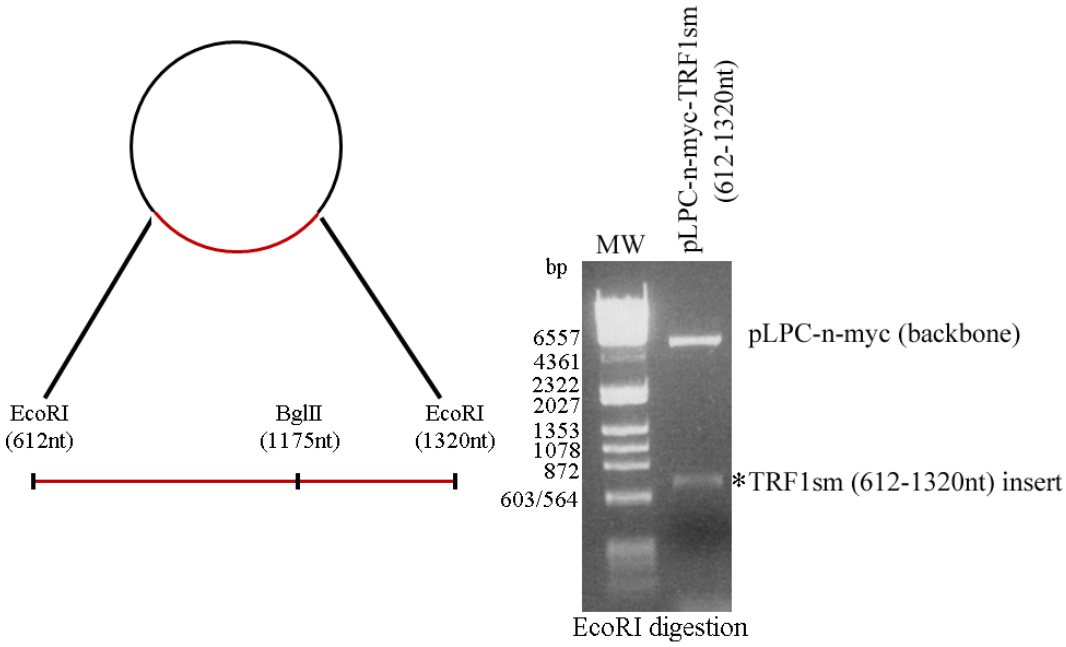
EcoRI
(612nt)
BglII
(1175nt)
EcoRI
(1320nt)
MW
pLPC-n-myc-TRF1sm
(612-1320nt)
bp
6557
4361
2322
2027
1353
1078
872
603/564
pLPC-n-myc (backbone)
*TRF1sm (612-1320nt) insert
EcoRI digestion

B

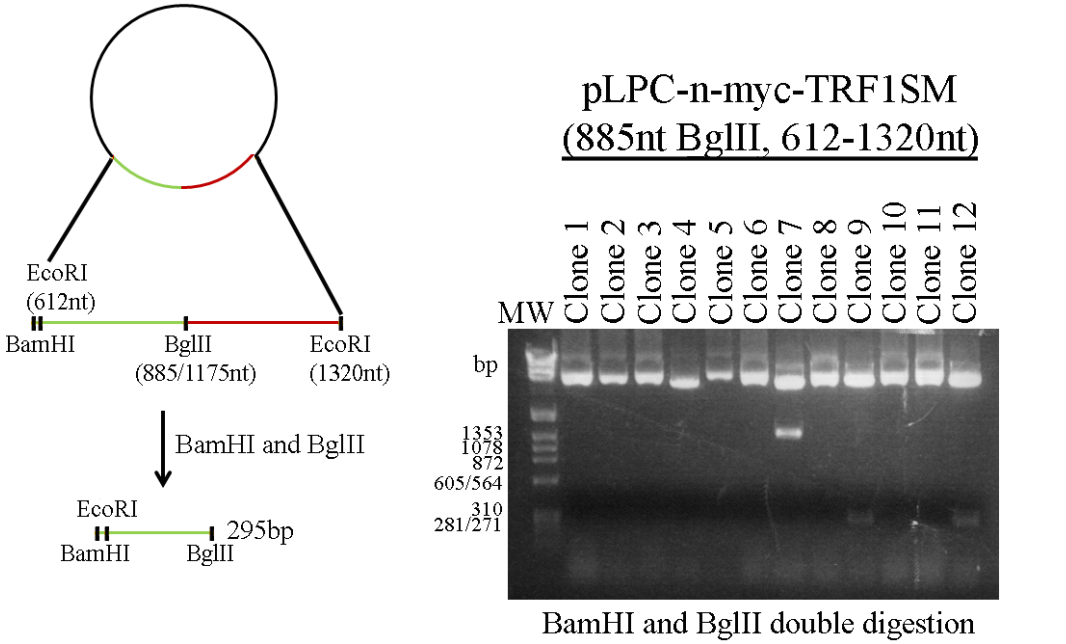
EcoRI
(612nt)
BamHI
BglII
(885/1175nt)
EcoRI
(1320nt)
BamHI and BglII
EcoRI
BamHI
BglII
295bp
pLPC-n-myc-TRF1SM
(885nt BglII, 612-1320nt)
MW
Clone 1
Clone 2
Clone 3
Clone 4
Clone 5
Clone 6
Clone 7
Clone 8
Clone 9
Clone 10
Clone 11
Clone 12
bp
1353
1078
872
605/564
310
281/271
BamHI and BglII double digestion

C1

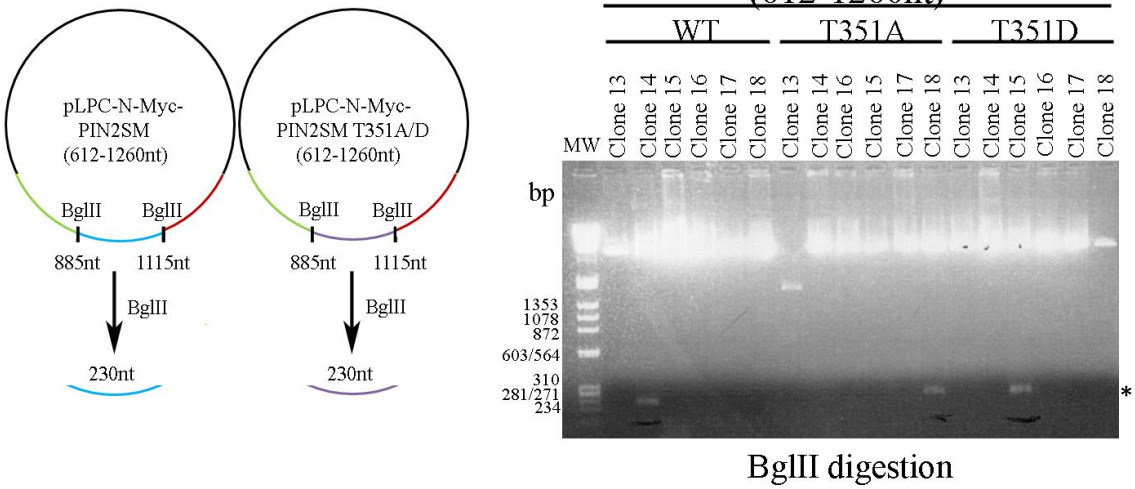
pLPC-N-Myc-PIN2SM (612-1260nt)
pLPC-N-Myc-PIN2SM (612-1260nt)
BglII
BglII
885nt
1115nt
BglII
230nt
pLPC-N-Myc-PIN2SM T351A/D (612-1260nt)
BglII
BglII
885nt
1115nt
BglII
230nt
pLPC-N-Myc-PIN2SM (612-1260nt)
WT
T351A
T351D
MW
Clone 13
Clone 14
Clone 15
Clone 16
Clone 17
Clone 18
bp
1353
1078
872
603/564
310
281/271
234
*
BglII digestion

C2

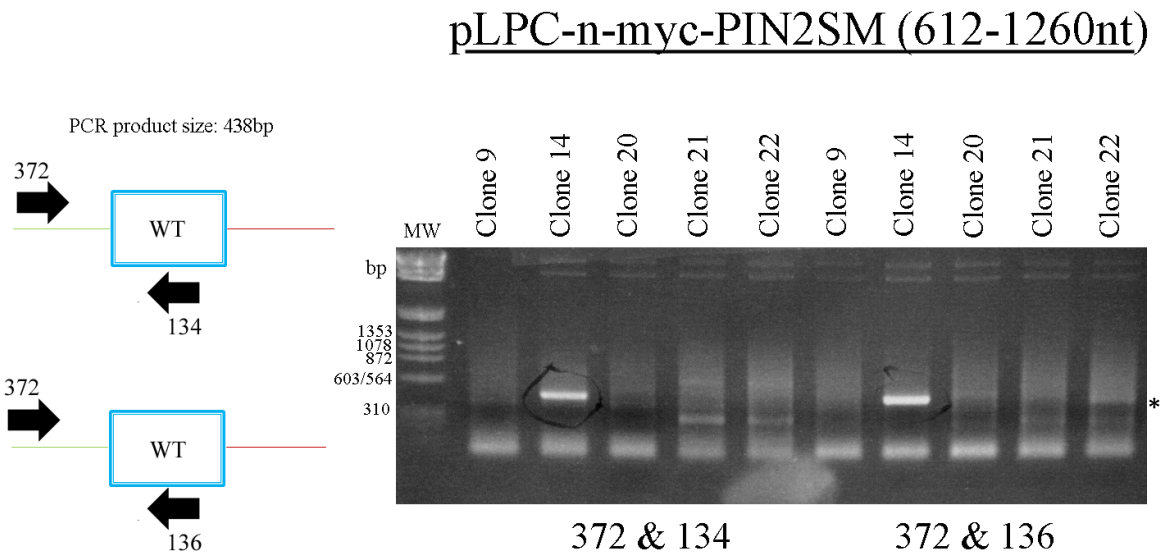
pLPC-n-myc-PIN2SM (612-1260nt)
PCR product size: 438bp
372
WT
134
372
WT
136
MW
Clone 9
Clone 14
Clone 20
Clone 21
Clone 22
Clone 9
Clone 14
Clone 20
Clone 21
Clone 22
bp
1353
1078
872
603/564
310
*
372 & 134
372 & 136

C3

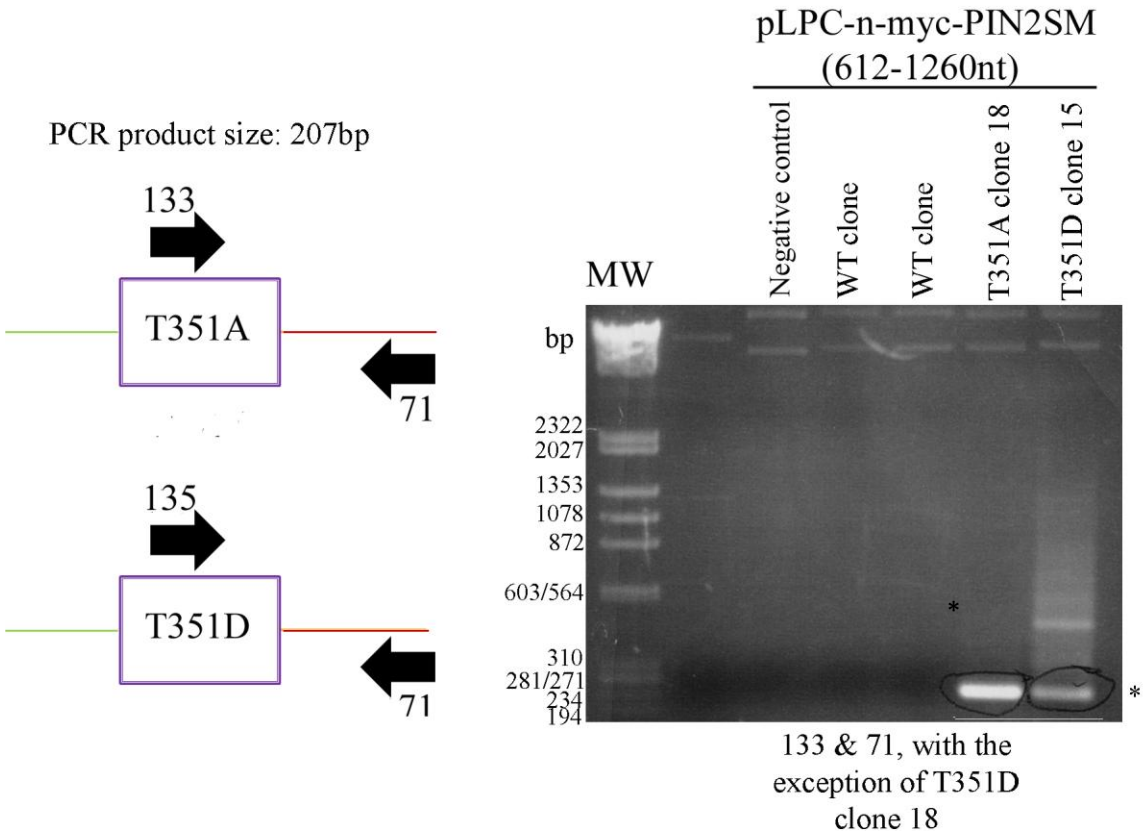

133 & 71, with the exception of T351D clone 18

D1

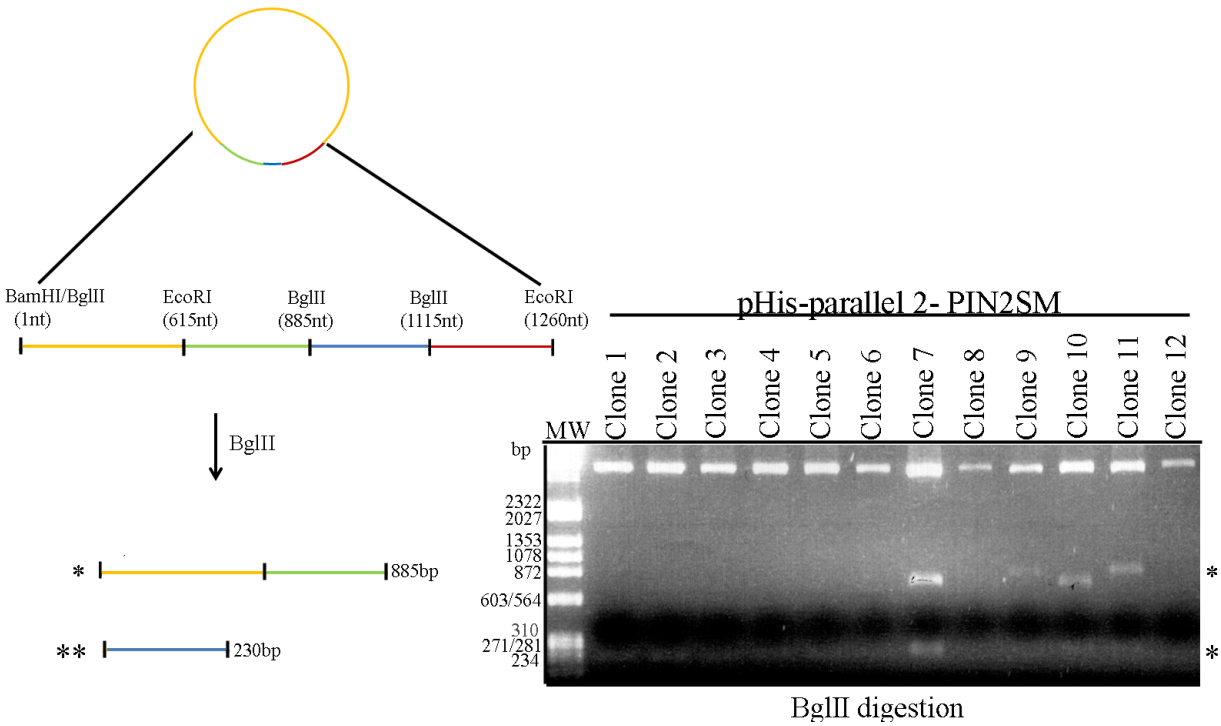

BglII digestion

D2

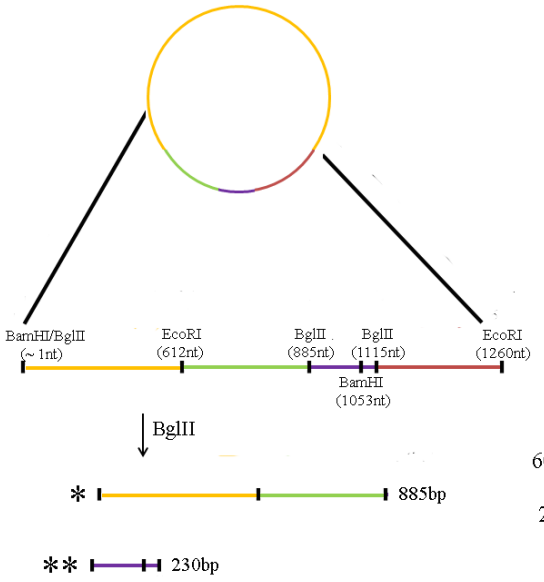
BamHI/BglII
(~ 1nt)
EcoRI
(612nt)
BglII
(885nt)
BglII
(1115nt)
EcoRI
(1260nt)
BamHI
(1053nt)
BglII
*
885bp
**
230bp

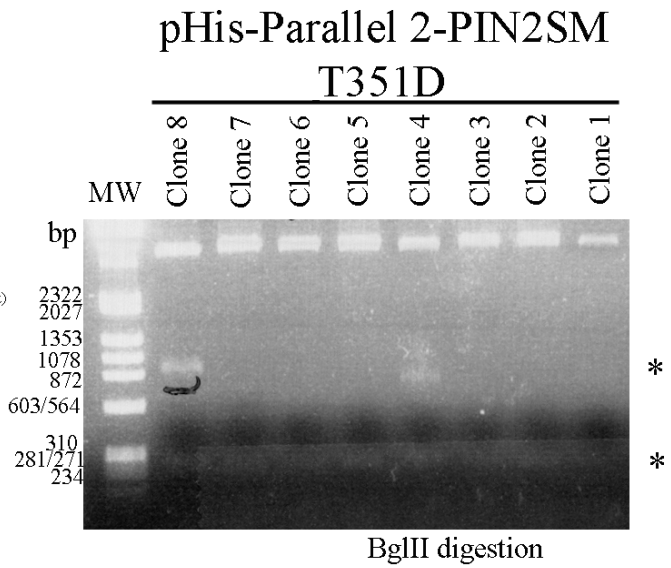
pHis-Parallel 2-PIN2SM
T351D
MW
Clone 8
Clone 7
Clone 6
Clone 5
Clone 4
Clone 3
Clone 2
Clone 1
bp
2322
2027
1353
1078
872
603/564
310
281/271
234
*
*
BglII digestion

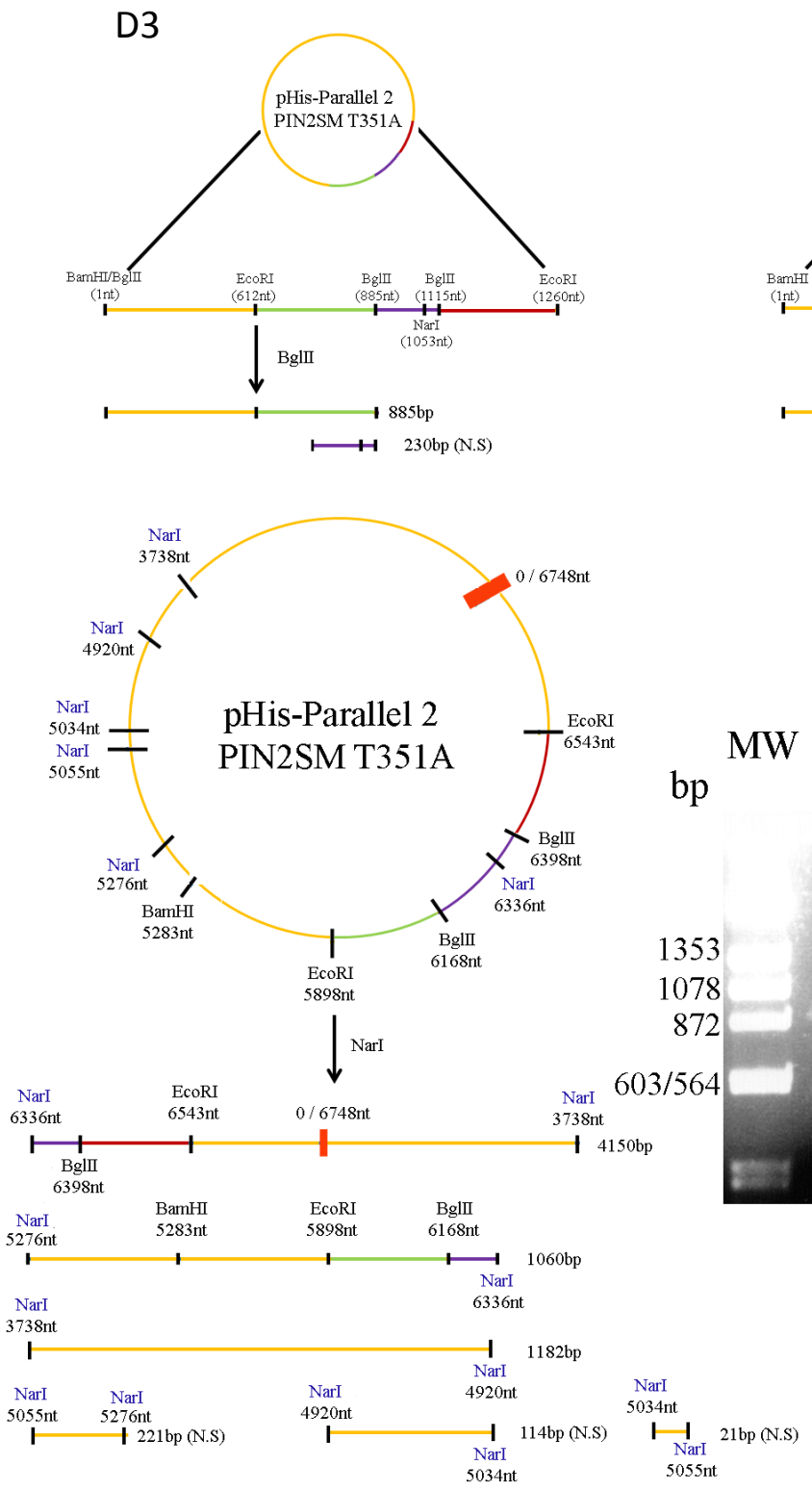
D3
pHis-Parallel 2
PIN2SM T351A
BamHI/BglII
(1nt)
EcoRI
(612nt)
BglII
(885nt)
BglII
(1115nt)
EcoRI
(1260nt)
NarI
(1053nt)
BglII
885bp
230bp (N.S)
pHis-Parallel 2
PIN2SM T351D
BamHI
(1nt)
EcoRI
(612nt)
BglII
(885nt)
BglII
(1115nt)
EcoRI
(1260nt)
BamHI
(1053nt)
BamHI
1053bp
pHis-Parallel 2
PIN2SM T351A
NarI
3738nt
0 / 6748nt
NarI
4920nt
NarI
5034nt
NarI
5055nt
EcoRI
6543nt
BglII
6398nt
NarI
6336nt
NarI
5276nt
BamHI
5283nt
BglII
6168nt
EcoRI
5898nt
NarI
NarI
6336nt
EcoRI
6543nt
0 / 6748nt
NarI
3738nt
4150bp
BglII
6398nt
NarI
5276nt
BamHI
5283nt
EcoRI
5898nt
BglII
6168nt
1060bp
NarI
6336nt
NarI
3738nt
1182bp
NarI
4920nt
NarI
5055nt
NarI
5276nt
221bp (N.S)
NarI
4920nt
114bp (N.S)
NarI
5034nt
NarI
5034nt
21bp (N.S)
NarI
5055nt
pHis-Parallel 2-Pin2SM
MW
bp
positive control
clone 11
negative control
clone 10
T351A clone 10
Clone 11
T351A clone 10
Clone 11
T351D clone 8
1353
1078
872
603/564
BglII
digestion
NarI
digestion
BamHI
digestion

Figure 3.2 (A) Schematic diagram of protein maps for His-TRF1, His-TRF1-T271A, His-TRF1-T271D, His-TRF1-S279A, His-TRF1-S279D, His-TRF1-T305A, His-TRF1-T305D, His-TRF1-T371A, His-TRF1-T371D, His-PIN2, His-PIN2 T351A, and His-PIN2 T351D. **(B)** Coomassie stained SDS-PAGE gel with 1µg of TRF1 and PIN2 proteins. Recombinant proteins were expressed in BL21 *pLysS*. Protein concentrations were verified through Bradford assay.

A

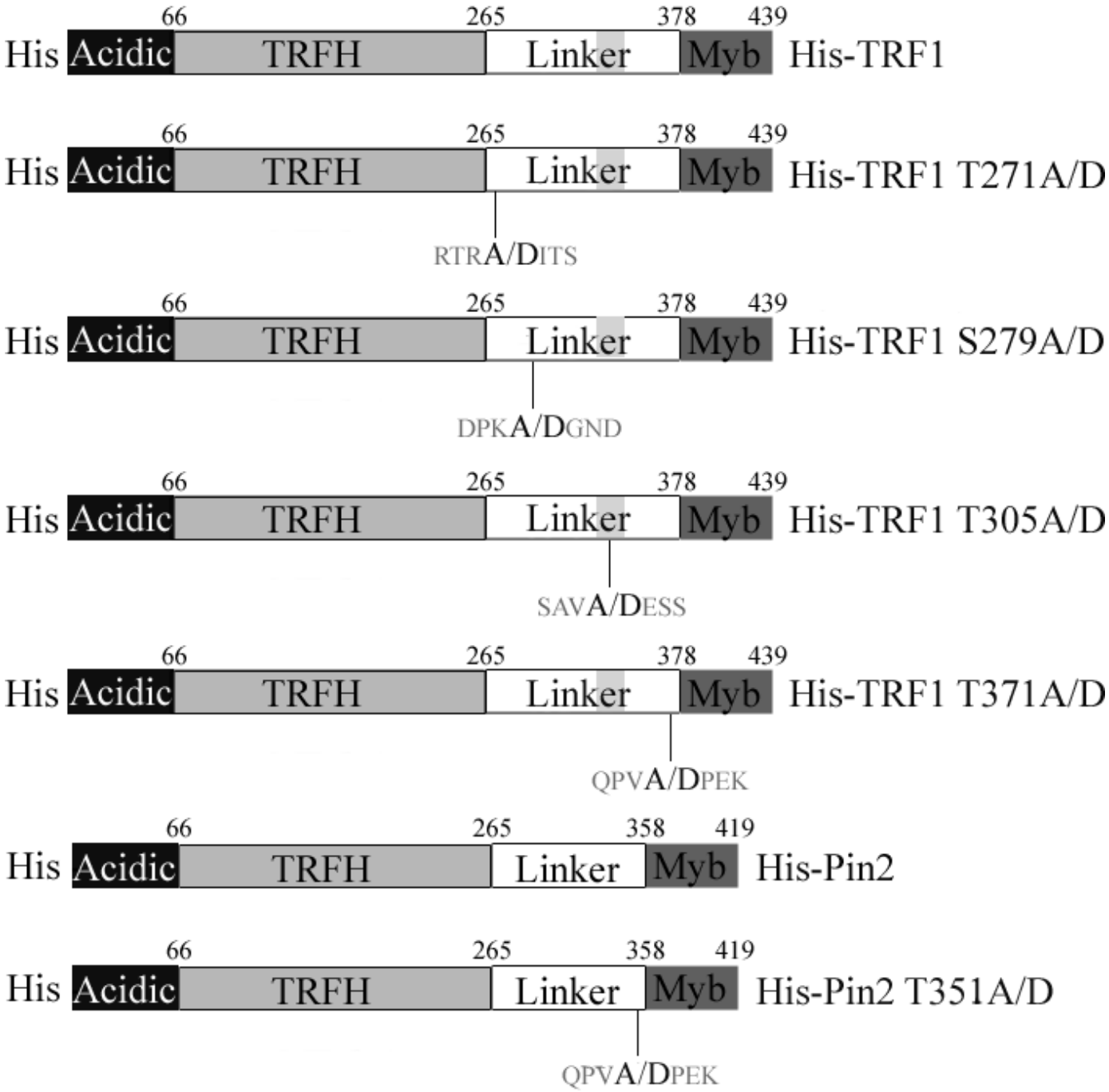
66
265
378
439
His
Acidic
TRFH
Linker
Myb
His-TRF1
His-TRF1 T271A/D
RTRA/DITS
His-TRF1 S279A/D
DPKA/DGND
His-TRF1 T305A/D
SAVA/DESS
His-TRF1 T371A/D
QPVA/DPEK
358
419
His-Pin2
His-Pin2 T351A/D
QPVA/DPEK

B

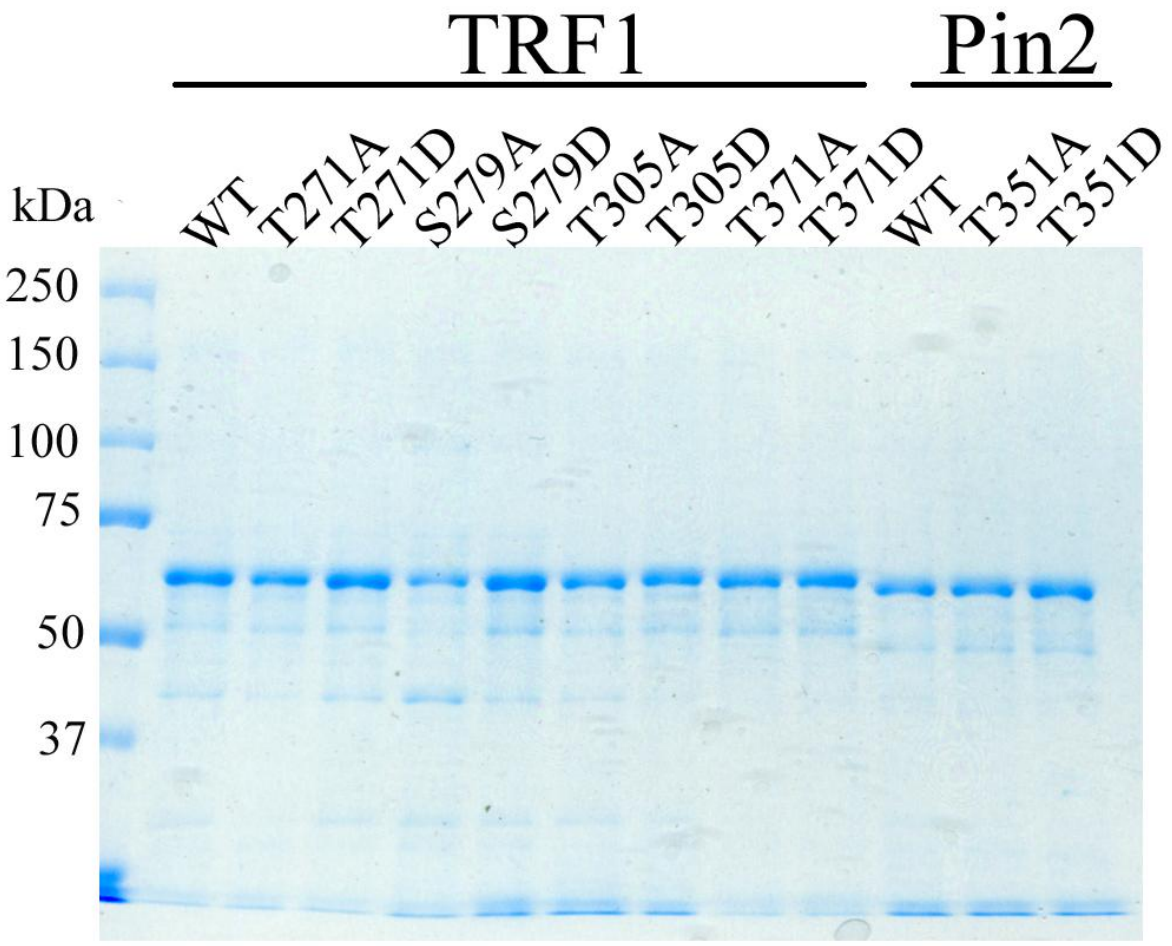
TRF1
Pin2
kDa
WT
T271A
T271D
S279A
S279D
T305A
T305D
T371A
T371D
WT
T351A
T351D
250
150
100
75
50
37

Figure 3.3 TRF1 mutants exhibit no binding defects under Gel shift condition 1. (**A)** Gel shift assay analyzing sites T271, S279, and T305. Samples were loaded at the indicated concentrations. The free probe lane serves as a control for unbound DNA. I, II, III indicate the binding complexes made between the recombinant TRF1 and telomeric substrate (188 bp). **(B- D)** Quantification of percentage of total DNA per lane converted to TRF1-DNA complexes. Standard deviations for TRF1 and TRF1 mutants were calculated from three independent experiments.

A

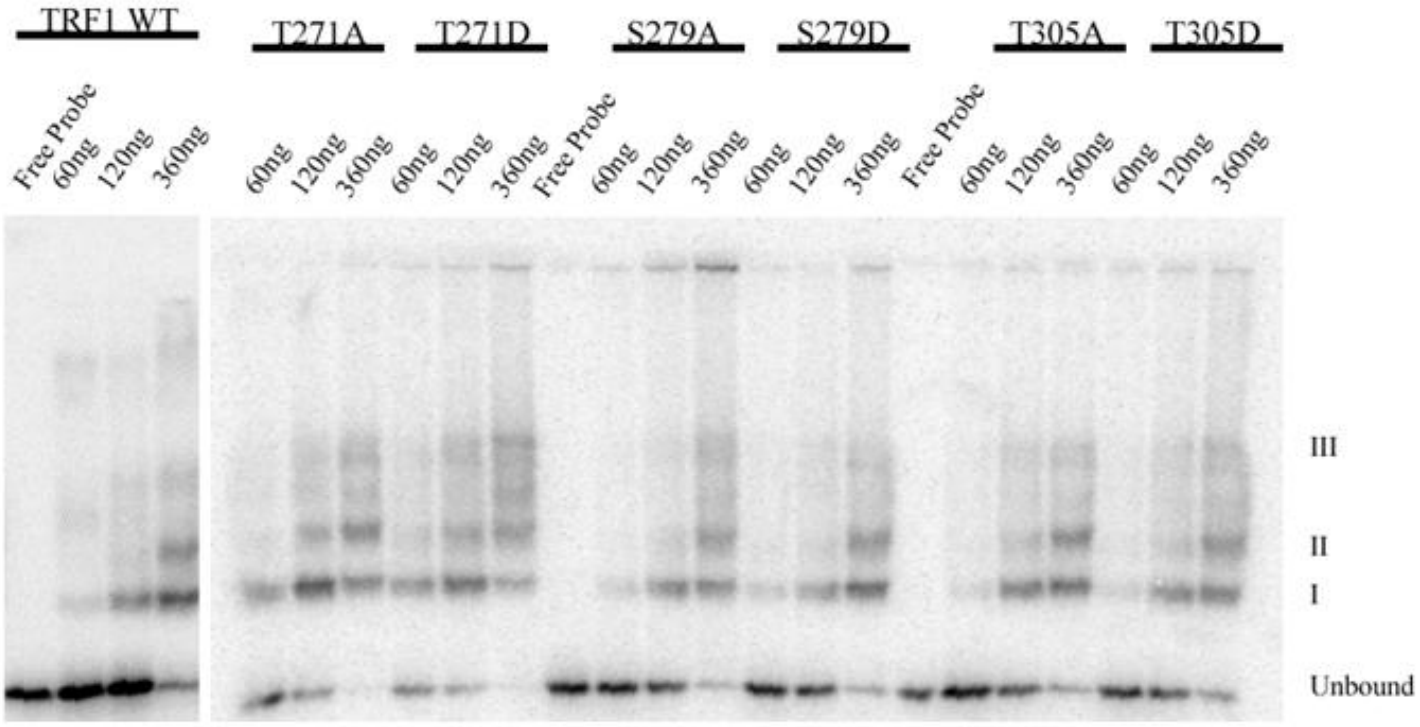
TRF1 WT
T271A
T271D
S279A
S279D
T305A
T305D
Free Probe
60ng
120ng
360ng
III
II
I
Unbound

B

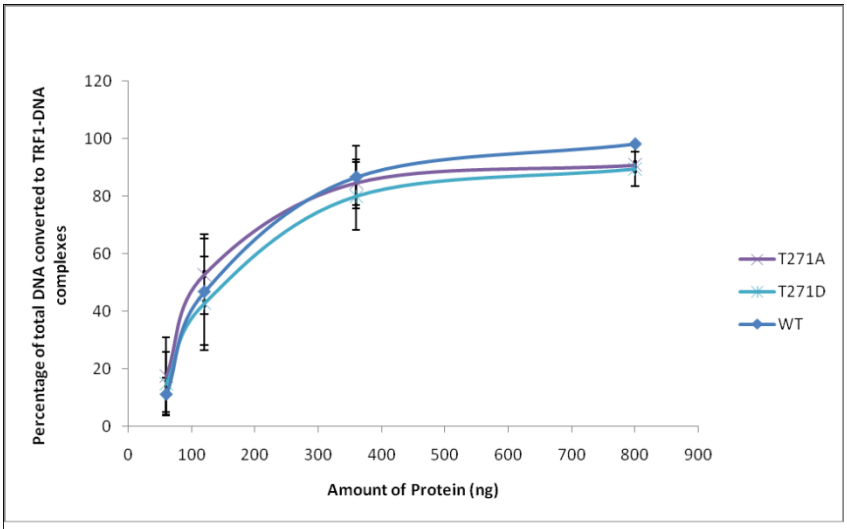
Percentage of total DNA converted to TRF1-DNA complexes
120
100
80
60
40
20
0
0
100
200
300
400
500
600
700
800
900
Amount of Protein (ng)
T271A
T271D
WT

C

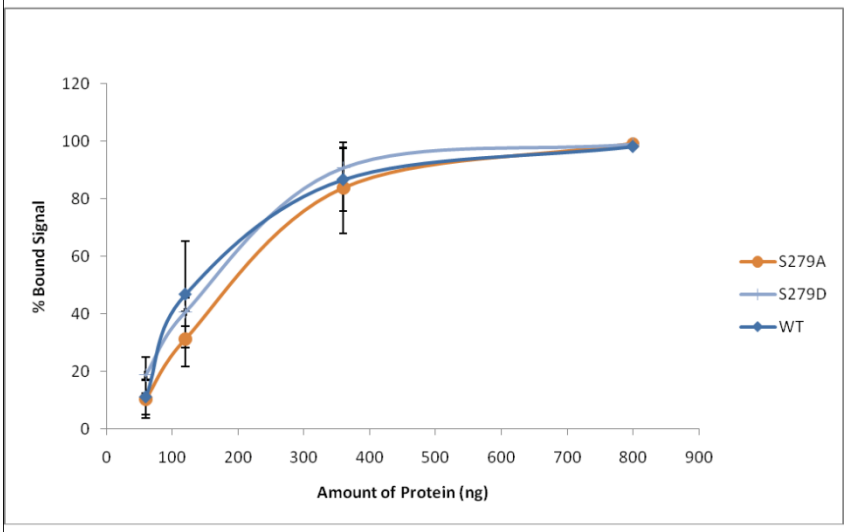
% Bound Signal
120
100
80
60
40
20
0
0
100
200
300
400
500
600
700
800
900
Amount of Protein (ng)
S279A
S279D
WT

D

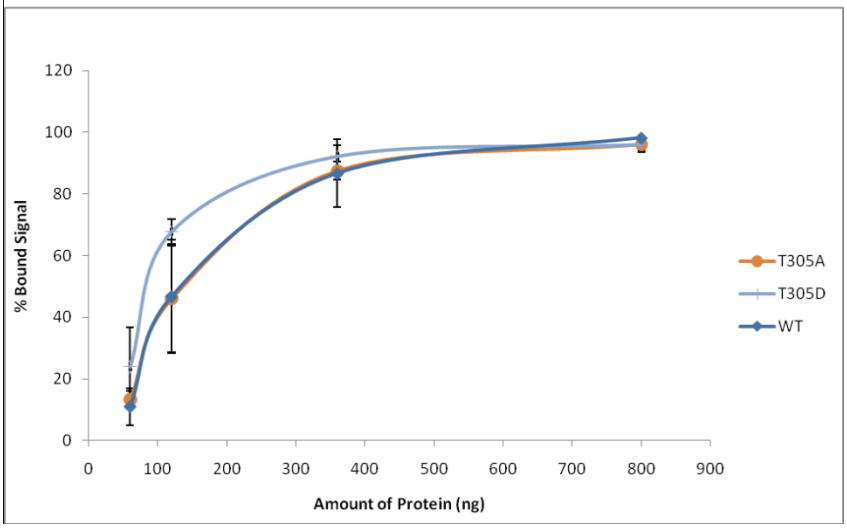
% Bound Signal
120
100
80
60
40
20
0
0
100
200
300
400
500
600
700
800
900
Amount of Protein (ng)
T305A
T305D
WT

Figure 3.4 Phosphomimic substitution of TRF1-T271 results in DNA binding defect under gel shift condition 2. Gel shift assays were conducted under condition 2 (70µg of BSA and 2µg of sheared *E. coli* DNA) comparing His-TRF1, phosphomimic, and alanine mutants. Samples were loaded at the indicated concentrations. The free probe lane serves as a control for unbound DNA. I, II, III indicate the binding complexes made between the recombinant TRF1 and telomeric substrate (188 bp). **A, C, E)** *In vitro* gel shift assays analyzing TRF1-S279A/D, T305A/D and T271A/D respectively. **B, D, F)** Quantification of percentage of total DNA per lane converted to TRF1-DNA complexes per lane. Standard deviations for TRF1 and TRF1 mutants were calculated from three independent experiments.

A

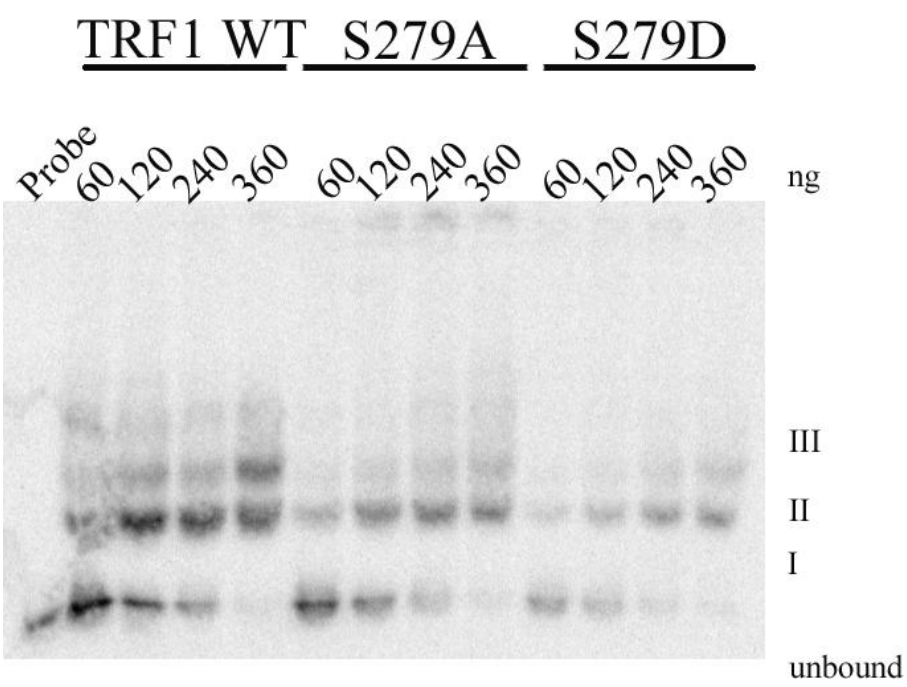
TRF1 WT S279A S279D
Probe
60 120 240 360 60 120 240 360 60 120 240 360
ng
III
II
I
unbound

B

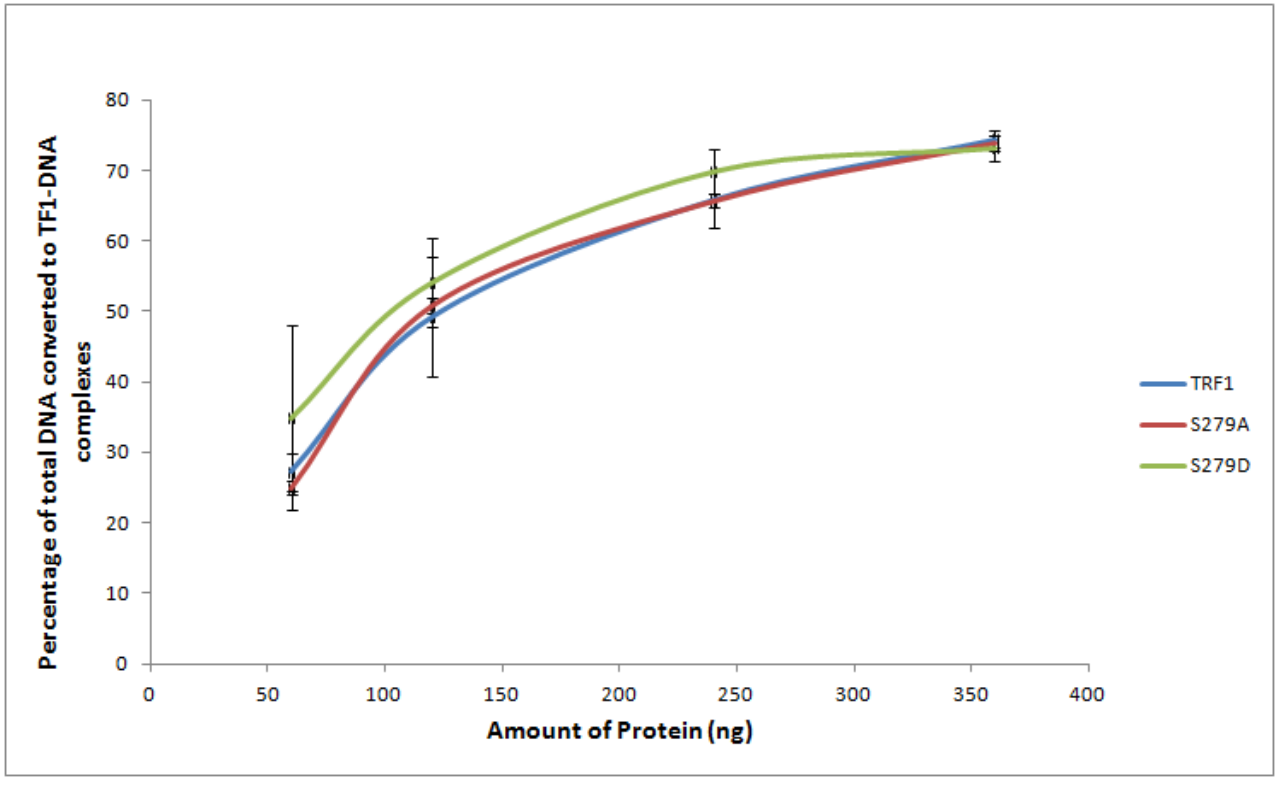
Percentage of total DNA converted to TF1-DNA complexes
0
10
20
30
40
50
60
70
80
0
50
100
150
200
250
300
350
400
Amount of Protein (ng)
TRF1
S279A
S279D

C

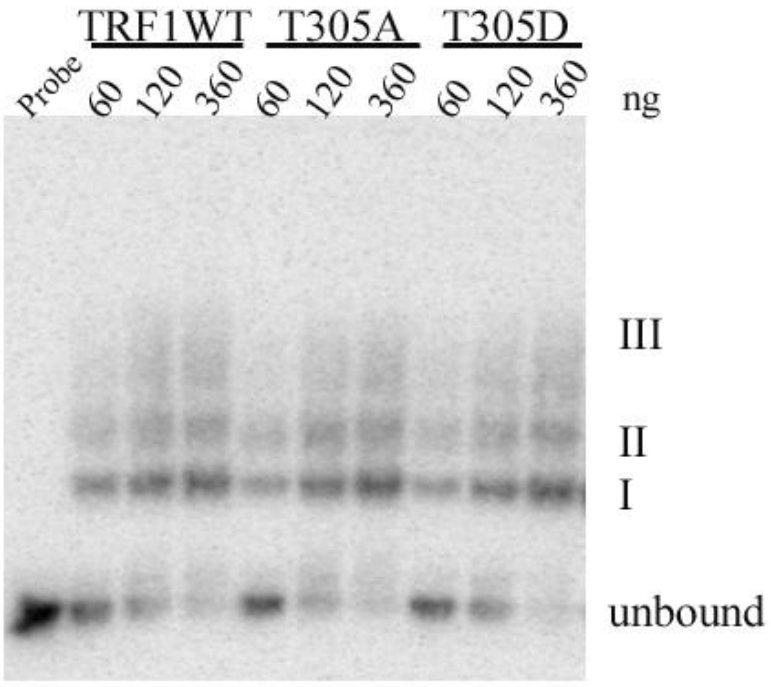
TRF1WT
T305A
T305D
Probe
60
120
360
60
120
360
60
120
360
ng
III
II
I
unbound

D

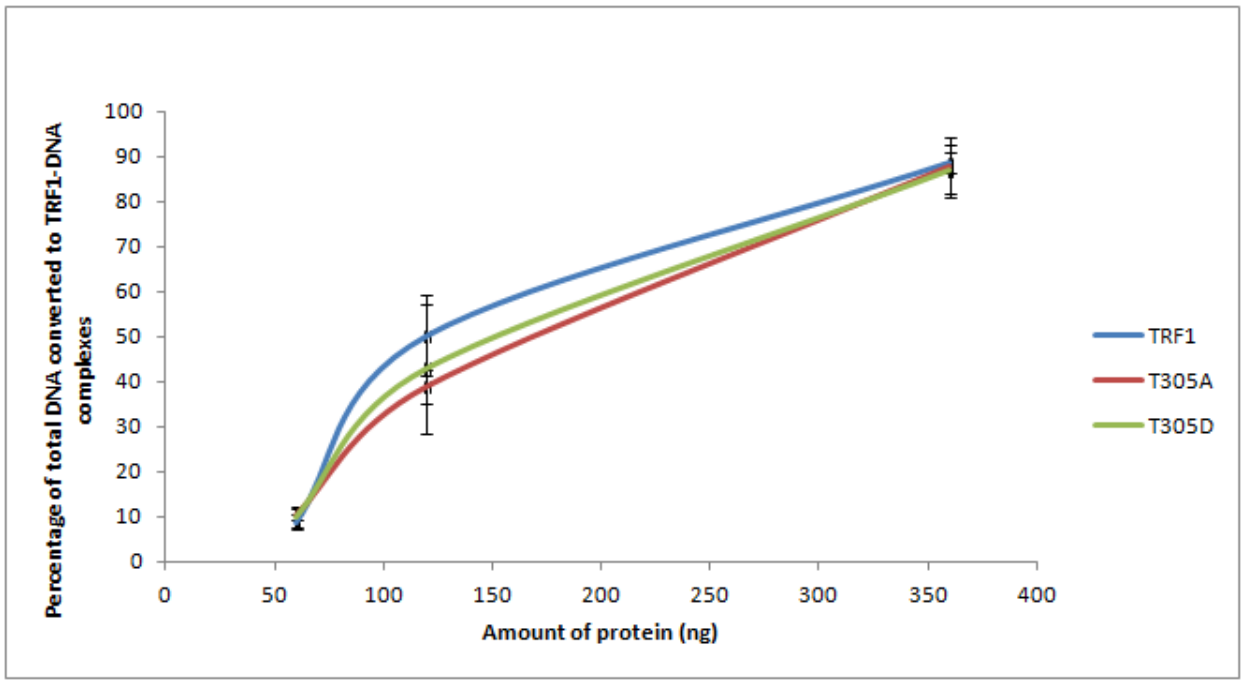
Percentage of total DNA converted to TRF1-DNA complexes
100
90
80
70
60
50
40
30
20
10
0
0
50
100
150
200
250
300
350
400
Amount of protein (ng)
TRF1
T305A
T305D

E

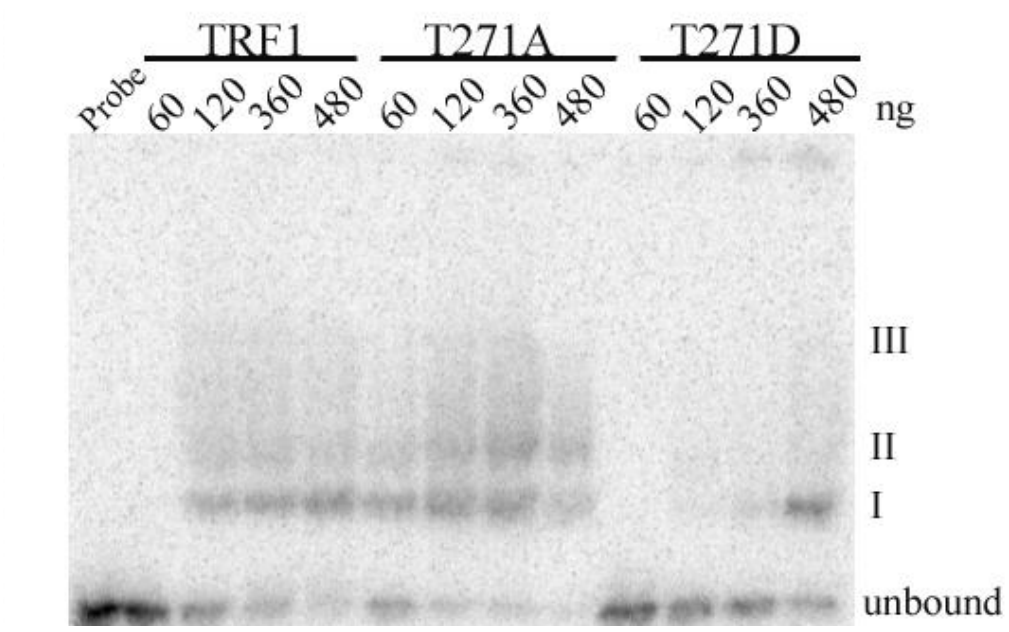
TRF1
T271A
T271D
Probe
60
120
360
480
60
120
360
480
60
120
360
480
ng
III
II
I
unbound

F

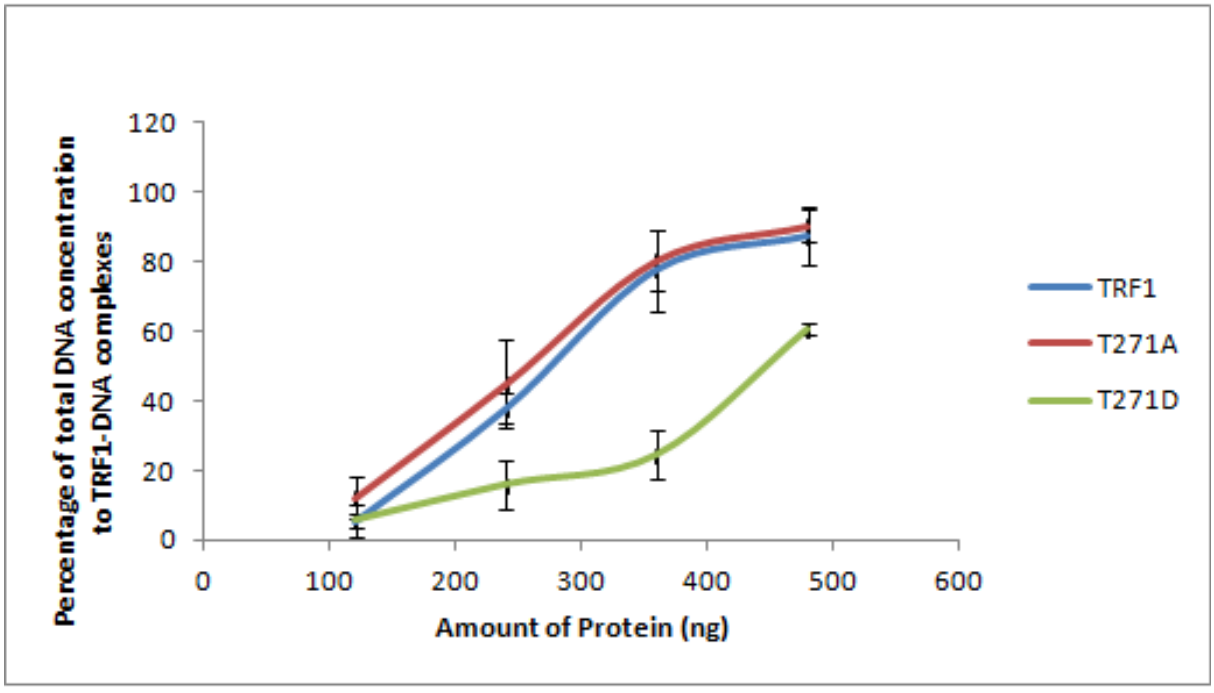
Percentage of total DNA concentration to TRF1-DNA complexes
120
100
80
60
40
20
0
0
100
200
300
400
500
600
Amount of Protein (ng)
TRF1
T271A
T271D

Figure 3.5 *In vitro* analysis comparing TRF1 and PIN2. **(A)** *In vitro* Cdk1 kinase assay showed a reduction in the phosphorylation of wild-type PIN2 and TRF1-T371A mutant compared to wild-type TRF1. Both the Coomassie stained gel (right panel and autoradiograph (left panel) are shown with the respective protein indicated above. The reduction in the phosphorylation of wild type PIN2 compared to wild type TRF1 was observed in two independent experiments. **(B)** Gel shift assay comparing his-PIN2, PIN2-T351A (alanine mutant) and PIN2-T351D (phosphomimic mutant). Samples were loaded in the indicated amount. **(C)** Quantification of percentage of total DNA per lane converted to PIN2-DNA complexes per lane. Standard deviations for PIN2 and PIN2 mutants were calculated from three independent experiments. **(D)** Gel shift assay comparing His-TRF1, TRF1-T371A (alanine mutant) and TRF1-T371D (phosphomimic mutant). The gel shift analysis of his-TRF1 and its T371 mutants is to serve as a control to ensure the reliability of the gel shift reagent by reproducing results from a published paper (McKerlie, 2011). It also serves as a way of highlighting the stark differences with the PIN2 counterparts. **(E)** Quantification of percentage of total DNA per lane converted to TRF1-DNA complexes per lane. Standard deviations were calculated from three independent experiments.

A

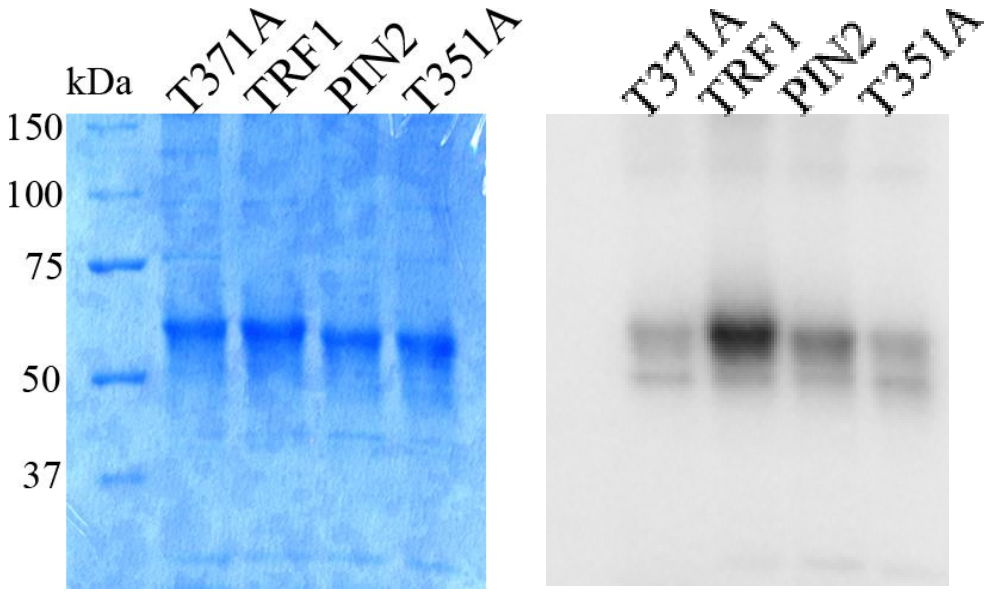
kDa
T371A
TRF1
PIN2
T351A
150
100
75
50
37
T371A
TRF1
PIN2
T351A

B

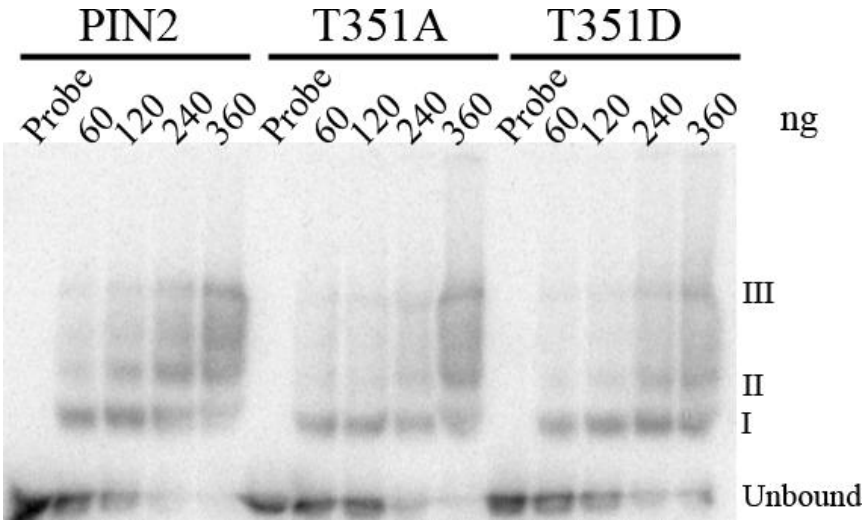
PIN2
T351A
T351D
Probe
60
120
240
360
ng
III
II
I
Unbound

C

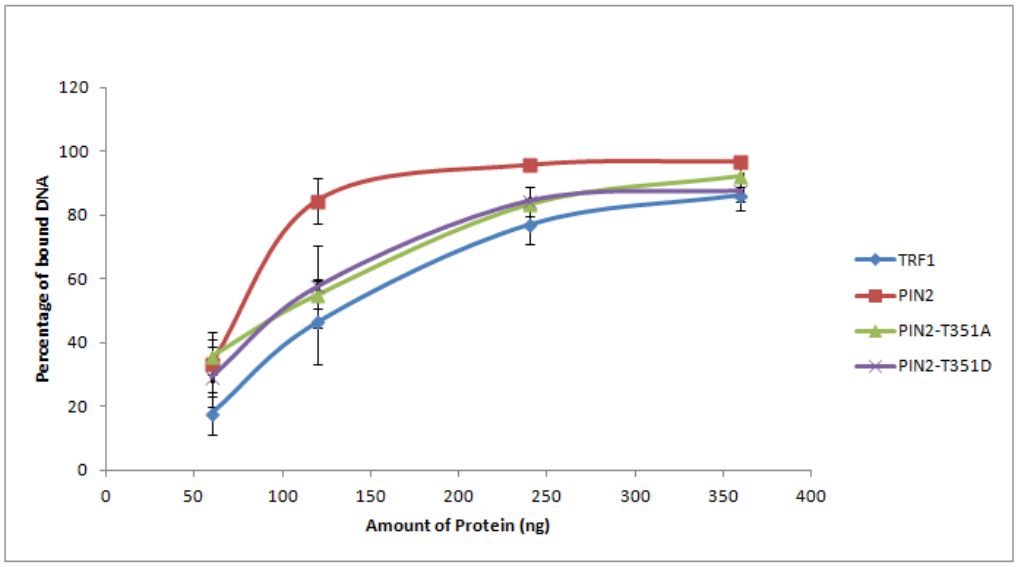
120
100
80
60
40
20
0
Percentage of bound DNA
0
50
100
150
200
250
300
350
400
Amount of Protein (ng)
TRF1
PIN2
PIN2-T351A
PIN2-T351D

D

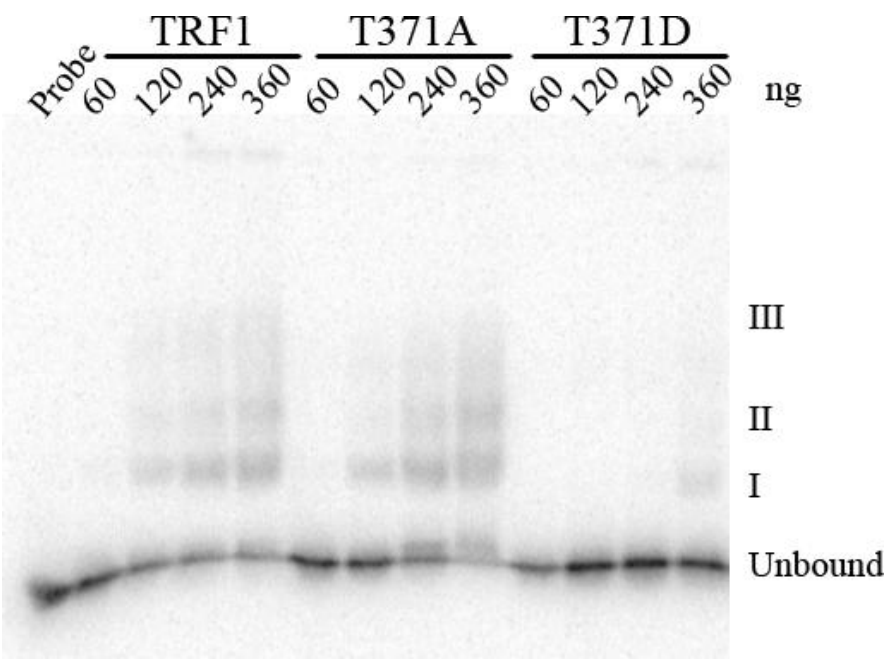
TRF1
T371A
T371D
Probe
60
120
240
360
60
120
240
360
60
120
240
360
ng
III
II
I
Unbound

E

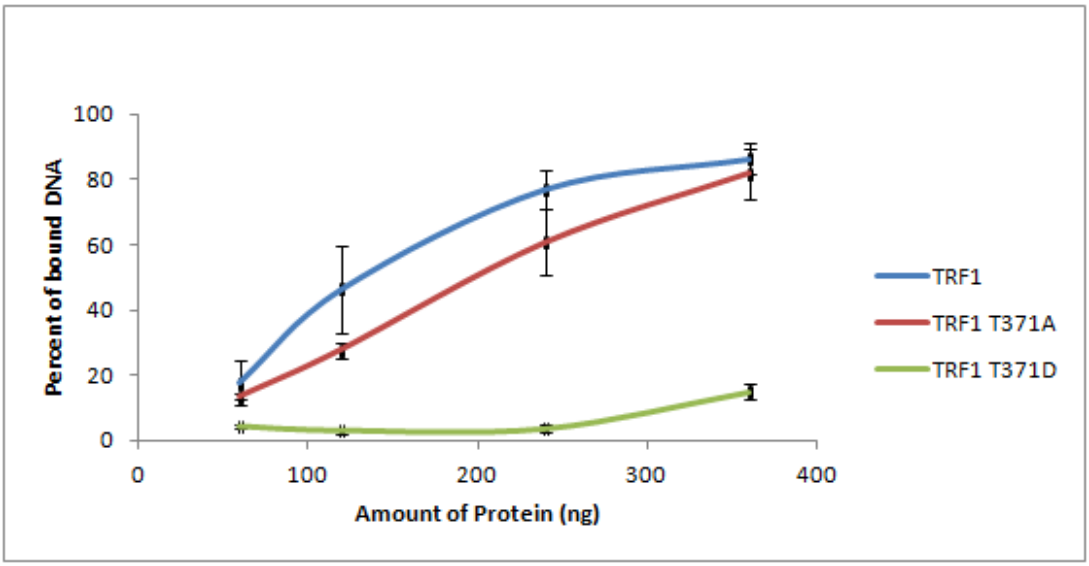
Percent of bound DNA
100
80
60
40
20
0
0
100
200
300
400
Amount of Protein (ng)
TRF1
TRF1 T371A
TRF1 T371D

Chapter 4 – Discussion

4.1 *In vitro* telomere binding assay of TRF1 phosphorylation sites T271, S279 and T305.

In this thesis, alanine and aspartic acid mutant recombinant proteins were used to characterize the telomeric DNA binding ability of phosphorylated TRF1. Through both types of *in vitro* gel shift conditions, TRF1 S279 and T305 mutants did not exhibit any DNA binding defects. However, TRF1-T271D was identified to have a DNA binding defect in comparison to TRF1-T271A and wild type TRF1 (Fig. 3.4 E,F). Although, TRF1-T271D mutant failed to show the defect under gel shift condition 1, the defect was observed in condition 2. My finding that TRF1-T271D exhibits a defect in binding to telomeric DNA in the presence of an increased amount of sheared *E. coli* DNA suggests that phosphorylation at T271 might render TRF1 a relaxed binding affinity for telomeric DNA. It has previously been reported through *in vitro* gel shift assay that the DNA binding defect of TRF1-S367D mutant were only seen under condition 2, suggesting that gel shift condition 1 is not always optimal to observe DNA binding defects of TRF1 (McKerlie *et al.,* 2012). On the other hand, TRF1-S367D mutant also exhibits a telomere elongation phenotype when complemented in a TRF1 deficient cell line (McKerlie *et al.,* 2012).The TRF1-S367D mutant complies with the general functional mechanism of TRF1, where a TRF1 DNA binding defect would result in its inability to prevent telomere elongation (McKerlie *et al.,* 2012; van Steensel and de Lange 1997). Although, I made attempts to address the role of T271 in telomere length maintenance. The data

appeared to be inconclusive and required further analysis that was not possible due to time constraints.

In addition, to telomere length maintenance analysis of TRF1 T271, it would also be interesting to see whether the phosphorylation at T271 would affect TRF1 dimerization. The T271 site is located on the N-terminal end of the linker region outside of the helix 9 motif of the dimerization domain which may suggest that phosphorylation at this site may result in a conformational change that would affect the oligomerization of TRF1, which can also result in DNA binding failure (Bianchi *et al.*, 1997; Fairall *et al.*, 2001). To address this possibility, a co-transfection of flag and myc tagged TRF1 T271 mutant followed by Co-IP should be conducted.

Although, mutational analysis of S279 and T305 did not yield any binding defects *in vitro*. The data is not sufficient to completely rule out the possibility that the phosphorylation at S279 and T305 affect telomere association *in vivo*. The *in vitro* gel shift assay consists of an interaction between a protein and naked substrate DNA (Reviewed by Hellman *et al.,* 2007). This oversimplifies and can potentially misrepresent the protein DNA complexes found in a cellular environment. In eukaryotic cells, telomeric DNA consists of the shelterin complex, and nucleosomes (Reviewed by Palm *et al.,* 2008; Cacchione *et al.,* 1997; Filesi *et al.,* 2000). The presence of nucleosomes at telomeres may act as a barrier to TRF1 S279 and T305 mutant binding. It has previously been reported that the introduction of nucleosomes on to naked telomeric DNA significantly reduced the percentage of TRF1-telomeric DNA complex compared to

just naked telomeric DNA (Galati *et al.,* 2006). It would be interesting to know whether the presence of histones would affect the DNA binding ability of S279 and T305 mutants; as the condition would more closely resemble the DNA environment of the cell. This can be addressed by conducting a ChIP using exogenously expressed TRF1 and TRF1 phosphorylation mutants to evaluate telomeric DNA interactions *in vivo*.

Potential phosphorylation sites S279 and T305 sites may influence TRF1 function independent of telomeric DNA binding. It has been reported that phosphorylation on TRF1 has affects on protein stability and turnover *in vivo* (McKerlie *et al.,* 2012; McKerlie *et al.,* 2011; Lee *et al.,* 2009; Kim *et al.,* 2008). Cyclohexamide treatment on cells exogenously expressing tagged wild type TRF1, phosphomimic and non-phosphorylatable mutants of S279 or T305 sites may reveal a role in TRF1 protein stability. Immunofluorescence analysis of tagged TRF1 mutants can also be conducted to determine whether any distinct foci are produced independent of telomere staining. Myc-IF analysis of cells expressing myc-TRF1 S367D proteins produced distinct foci which were heterogeneous in size and sensitive to proteosome inhibitors (McKerlie *et al.,* 2012). Another aspect of TRF1 phosphorylation function independent of telomere binding involves its role in DNA damage response (Kishi *et al.,* 2001). It has been reported that ATM deficient cell lines expressing exogenous TRF1 S219D proteins lose their sensitivity to IR treatment, which was observed through the decrease in apoptosis frequency (Kishi *et al.,* 2001). It would be interesting to see whether phosphomimic and non-phosphorylatable S279 and T305 TRF1 mutants would affect IR sensitivity in AT cells. It would be particularly interesting to conduct these experiments on potential

phosphorylation site TRF1 T305 since this residue is absent in PIN2. Any functional roles identified with T305 would be an exclusive and distinct role found in TRF1 and not PIN2.

4.2 *In vitro* characterization of TRF1 and PIN2 mutant constructs

CDK1 kinase assays revealed that PIN2 is phosphorylated at T351. This was observed as a slight reduction in the phosphorylation level of PIN2-T351A mutant compared to PIN2 wild type (Fig. 3.5A). This is consistent with a previous report that shows that CDK1 phosphorylates TRF1-T371 (McKerlie, 2011; Fig 3.5A). I also showed that CDK1 net phosphorylation of PIN2 is significantly lower than the phosphorylation level of TRF1 (Fig 3.5A). The lower net phosphorylation of PIN2 by CDK1 may be due to the possibility that TRF1 has non-specific phosphorylation modification sites *in vitro*. It has been documented that recombinant kinases can phosphorylate substrate proteins indiscriminately which may explain why TRF1 phosphorylation levels are higher compared its isoform, PIN2 (Reviewed by Lienhard, 2008). However, if this is not the case, then it would be of great interest to identify CDK1 dependent TRF1 and PIN2 phosphorylation sites. This can be done by conducting a CDK1 *in vitro* kinase assay using cold ATP on TRF1 and PIN2 respectively, followed by mass spectrometry. By identifying additional CDK1 phosphorylation sites on TRF1 and PIN2, we can begin to address the functional role of these other sites. It would also be interesting to characterize and look at the difference in CDK1 phosphorylation sites and function between PIN2 and TRF1.

In vitro gel shift assays performed on PIN2 T351 mutants show that there is no binding defect associated with this site compared to the severe DNA binding defect observed in TRF1 T371D mutant (Fig. 3.5B-E). Based off of what has already been known about the latter of phosphomimic introduction at T371, it is important to address the possibility of whether the PIN2 T351D mutant is behaving like a phosphomimic. In order to address this possibility, a CDK1 kinase assay followed by a gel shift assay should be conducted comparing PIN2 and TRF1. If the phosphorylation at PIN2 T351 results in no binding defect then it would confirm the result observed in PIN2 T351D gel shift assay. If this holds true, the next logical approach is to assess the PIN2 T351 mutants in a PIN2 deficient cell line to determine whether any of the TRF1 T371 mutant phenotypes can be recapitulated.

Bibliography

References

Allshire, R. C., Gosden, J. R., Cross, S. H., Cranston, G., Rout, D., Sugawara, N., . . . Hastie, N. D. (1988). Telomeric repeat from T. thermophila cross hybridizes with human telomeres. *Nature, 332*(6165), 656-659. doi:10.1038/332656a0

Ancelin, K., Brunori, M., Bauwens, S., Koering, C. E., Brun, C., Ricoul, M., . . . Gilson, E. (2002). Targeting assay to study the cis functions of human telomeric proteins: Evidence for inhibition of telomerase by TRF1 and for activation of telomere degradation by TRF2. *Molecular and Cellular Biology*, *22*(10), 3474-3487.

Bae, N. S., & Baumann, P. (2007). A RAP1/TRF2 complex inhibits nonhomologous end-joining at human telomeric DNA ends. *Molecular Cell*, *26*(3), 323-334.

Baumann, P., & Cech, T. R. (2001). Pot1, the putative telomere end-binding protein in fission yeast and humans. *Science, 292*(5519), 1171-1175.

Baumgartner, B. L., & Lundblad, V. (2005). Telomere identity crisis. *Genes & Development*, *19*(21), 2522-2525.

Bianchi, A., Smith, S., Chong, L., Elias, P., & De Lange, T. (1997). TRF1 is a dimer and bends telomeric DNA. *The EMBO Journal*, *16*(7), 1785-1794.

Bianchi, A., Stansel, R. M., Fairall, L., Griffith, J. D., Rhodes, D., & de Lange, T. (1999). TRF1 binds a bipartite telomeric site with extreme spatial flexibility. *The EMBO Journal*, *18*(20), 5735-5744.

Bilaud, T., Brun, C., Ancelin, K., Koering, C. E., Laroche, T., & Gilson, E. (1997). Telomeric localization of TRF2, a novel human telobox protein. *Nature Genetics*, *17*(2), 236-239.

Blackburn, E. H., & Gall, J. G. (1978). A tandemly repeated sequence at the termini of the extrachromosomal ribosomal RNA genes in tetrahymena. *J Mol Biol*, *120*(1), 33-53.

Bodnar, A. G., Ouellette, M., Frolkis, M., Holt, S. E., Chiu, C. P., Morin, G. B., . . . Wright, W. E. (1998). Extension of life-span by introduction of telomerase into normal human cells. *Science*, *279*(5349), 349-352.

Broccoli, D., Smogorzewska, A., Chong, L., & De Lange, T. (1997). Human telomeres contain two distinct myb-related proteins, TRF1 and TRF2. *Nature Genetics*, *17*(2), 231-235.

Broccoli, D., Young, J. W., & de Lange, T. (1995). Telomerase activity in normal and malignant hematopoietic cells. *Proceedings of the National Academy of Sciences*, *92*(20), 9082.

Cacchione, S., Cerone, M. A., & Savino, M. (1997). In vitro low propensity to form nucleosomes of four telomeric sequences. *FEBS Letters, 400*(1), 37-41.

Celli, G. B., & de Lange, T. (2005). DNA processing is not required for ATM-mediated telomere damage response after TRF2 deletion. *Nature Cell Biology, 7*(7), 712-718.

Chang, W., Dynek, J. N., & Smith, S. (2003). TRF1 is degraded by ubiquitin-mediated proteolysis after release from telomeres. *Genes & Development, 17*(11), 1328-1333.

Chen, Y. C., Teng, S. C., & Wu, K. J. (2009). Phosphorylation of telomeric repeat binding factor 1 (TRF1) by akt causes telomere shortening. *Cancer Investigation, 27*(1), 24-28.

Cheng, J. F., Smith, C. L., & Cantor, C. R. (1989). Isolation and characterization of a human telomere. *Nucleic Acids Research, 17*(15), 6109-6127.

Chiu, C. P., Dragowska, W., Kim, N. W., Vaziri, H., Yui, J., Thomas, T. E., . . . Lansdorp, P. M. (1996). Differential expression of telomerase activity in hematopoietic progenitors from adult human bone marrow. *Stem Cells, 14*(2), 239-248.

Counter, C. M., Avilion, A. A., LeFeuvre, C. E., Stewart, N. G., Greider, C. W., Harley, C. B., & Bacchetti, S. (1992). Telomere shortening associated with chromosome

instability is arrested in immortal cells which express telomerase activity. *The EMBO Journal, 11*(5), 1921.

de Lange, T. (2005). Shelterin: The protein complex that shapes and safeguards human telomeres. *Genes & Development, 19*(18), 2100.

de Lange, T., Shiue, L., Myers, R. M., Cox, D. R., Naylor, S. L., Killery, A. M., & Varmus, H. E. (1990). Structure and variability of human chromosome ends. *Molecular and Cellular Biology, 10*(2), 518-527.

Denchi, E. L., & De Lange, T. (2007). Protection of telomeres through independent control of ATM and ATR by TRF2 and POT1. *Nature, 448*(7157), 1068-1071.

Dynek, J. N., & Smith, S. (2004). Resolution of sister telomere association is required for progression through mitosis. *Science, 304*(5667), 97-100.

Fairall, L., Chapman, L., Moss, H., de Lange, T., & Rhodes, D. (2001). Structure of the TRFH dimerization domain of the human telomeric proteins TRF1 and TRF2. *Molecular Cell, 8*(2), 351-361.

Feng, J., Funk, W. D., Wang, S. S., Weinrich, S. L., Avilion, A. A., Chiu, C. P., . . . Yu, J. (1995). The RNA component of human telomerase. *Science, 269*(5228), 1236.

Filesi, I., Cacchione, S., De Santis, P., Rossetti, L., & Savino, M. (2000). The main role of the sequence-dependent DNA elasticity in determining the free energy of

nucleosome formation on telomeric DNAs. *Biophysical Chemistry, 83*(3), 223-237.

Galati, A., Rossetti, L., Pisano, S., Chapman, L., Rhodes, D., Savino, M., & Cacchione, S. (2006). The human telomeric protein TRF1 specifically recognizes nucleosomal binding sites and alters nucleosome structure. *Journal of Molecular Biology, 360*(2), 377-385.

Gilson, E., & Géli, V. (2007). How telomeres are replicated. *Nature Reviews Molecular Cell Biology, 8*(10), 825-838.

Greider, C. W., & Blackburn, E. H. (1985). Identification of a specific telomere terminal transferase activity in tetrahymena extracts. *Cell, 43*(2 Pt 1), 405-413.

Griffith, J. D., Comeau, L., Rosenfield, S., Stansel, R. M., Bianchi, A., Moss, H., & De Lange, T. (1999). Mammalian telomeres end in a large duplex loop. *CELL-CAMBRIDGE MA-, 97*, 503-514.

Hanaoka, S., Nagadoi, A., & Nishimura, Y. (2005). Comparison between TRF2 and TRF1 of their telomeric DNA-bound structures and DNA-binding activities. *Protein Science, 14*(1), 119-130.

Hanish, J. P., Yanowitz, J. L., & de Lange, T. (1994). Stringent sequence requirements for the formation of human telomeres. *Proceedings of the National Academy of Sciences, 91*(19), 8861.

Harley, C. B. (1991). Telomere loss: Mitotic clock or genetic time bomb? *Mutation Research/DNAging, 256*(2), 271-282.

Harley, C. B., Futcher, A. B., & Greider, C. W. (1990). Telomeres shorten during ageing of human fibroblasts.

Harrington, L., Zhou, W., McPhail, T., Oulton, R., Yeung, D. S. K., Mar, V., . . . Robinson, M. O. (1997). Human telomerase contains evolutionarily conserved catalytic and structural subunits. *Genes & Development, 11*(23), 3109-3115.

Hayflick, L. (1961). The establishment of a line (WISH) of human amnion cells in continuous cultivation. *Experimental Cell Research, 23*(1), 14-20.

Hayflick, L. (1965). THE LIMITED IN ‘c/ITRO LIFETIME OF HUMAN DIPLOID CELL STRAINS1, 2. *Experimental Cell Research, 37*, 614-636.

Hellman, L. M., & Fried, M. G. (2007). Electrophoretic mobility shift assay (EMSA) for detecting protein–nucleic acid interactions. *Nature Protocols, 2*(8), 1849-1861.

Hockemeyer, D., Palm, W., Else, T., Daniels, J. P., Takai, K. K., Ye, J. Z. S., . . . Hammer, G. D. (2007). Telomere protection by mammalian Pot1 requires interaction with Tpp1. *Nature Structural & Molecular Biology, 14*(8), 754-761.

Houghtaling, B. R., Cuttonaro, L., Chang, W., & Smith, S. (2004). A dynamic molecular link between the telomere length regulator TRF1 and the chromosome end protector TRF2. *Current Biology, 14*(18), 1621-1631.

Iwatsuki, N., & Okazaki, R. (1967). Mechanism of regulation of deoxythymidine kinase of escherichia coli* 1:: II. effect of temperature on the enzyme activity and kinetics. *Journal of Molecular Biology, 29*(1), 155-165.

Karlseder, J., Broccoli, D., Dai, Y., Hardy, S., & de Lange, T. (1999). p53-and ATM-dependent apoptosis induced by telomeres lacking TRF2. *Science, 283*(5406), 1321-1325.

Karlseder, J., Kachatrian, L., Takai, H., Mercer, K., Hingorani, S., Jacks, T., & De Lange, T. (2003). Targeted deletion reveals an essential function for the telomere length regulator Trf1. *Molecular and Cellular Biology, 23*(18), 6533-6541.

Kilian, A., Bowtell, D. D. L., Abud, H. E., Hime, G. R., Venter, D. J., Keese, P. K., . . . Jefferson, R. A. (1997). Isolation of a candidate human telomerase catalytic subunit gene, which reveals complex splicing patterns in different cell types. *Human Molecular Genetics, 6*(12), 2011-2019.

Kim, H., Lee, O. H., Xin, H., Chen, L. Y., Qin, J., Chae, H. K., . . . Songyang, Z. (2009). TRF2 functions as a protein hub and regulates telomere maintenance by recognizing specific peptide motifs. *Nature Structural & Molecular Biology, 16*(4), 372-379.

Kim, M. K., Kang, M. R., Nam, H. W., Bae, Y. S., Kim, Y. S., & Chung, I. K. (2008). Regulation of telomeric repeat binding factor 1 binding to telomeres by casein

kinase 2-mediated phosphorylation. *Journal of Biological Chemistry, 283*(20), 14144.

Kim, S., Beausejour, C., Davalos, A. R., Kaminker, P., Heo, S. J., & Campisi, J. (2004). TIN2 mediates functions of TRF2 at human telomeres. *Journal of Biological Chemistry, 279*(42), 43799-43804.

Kim, S., Kaminker, P., & Campisi, J. (1999). TIN2, a new regulator of telomere length in human cells. *Nat Genet, 23*(4), 405-412.

Kishi, S., & Lu, K. P. (2002). A critical role for Pin2/TRF1 in ATM-dependent regulation. *Journal of Biological Chemistry, 277*(9), 7420-7429.

Kishi, S., Wulf, G., Nakamura, M., & Lu, K. P. (2001). Telomeric protein Pin2/TRF1 induces mitotic entry and apoptosis in cells with short telomeres and is down-regulated in human breast tumors. *Oncogene, 20*(12), 1497.

Kishi, S., Zhou, X. Z., Ziv, Y., Khoo, C., Hill, D. E., Shiloh, Y., & Lu, K. P. (2001). Telomeric protein Pin2/TRF1 as an important ATM target in response to double strand DNA breaks. *Journal of Biological Chemistry, 276*(31), 29282-29291.

Konishi, A., & De Lange, T. (2008). Cell cycle control of telomere protection and NHEJ revealed by a ts mutation in the DNA-binding domain of TRF2. *Genes & Development, 22*(9), 1221.

Kruk, P. A., Rampino, N. J., & Bohr, V. A. (1995). DNA damage and repair in telomeres: Relation to aging. *Proceedings of the National Academy of Sciences, 92*(1), 258.

Lages, CS., Etienne, O., Comte, J., Gauthier, L. R., Granotier, C., Pennarun, G., & Boussin, F. D. (2004). Identification of alternative transcripts of the TRF1/Pin2 gene. *Journal of Cellular Biochemistry, 93*(5), 968-979.

Lee, T. H., Perrem, K., Harper, J. W., Lu, K. P., & Zhou, X. Z. (2006). The F-box protein FBX4 targets PIN2/TRF1 for ubiquitin-mediated degradation and regulates telomere maintenance. *Journal of Biological Chemistry, 281*(2), 759-768.

Lee, T. H., Tun-Kyi, A., Shi, R., Lim, J., Soohoo, C., Finn, G., . . . Zhou, X. Z. (2008). Essential role of Pin1 in the regulation of TRF1 stability and telomere maintenance. *Nature Cell Biology, 11*(1), 97-105.

Lei, M., Podell, E. R., & Cech, T. R. (2004). Structure of human POT1 bound to telomeric single-stranded DNA provides a model for chromosome end-protection. *Nature Structural & Molecular Biology, 11*(12), 1223-1229.

Li, B., Oestreich, S., & de Lange, T. (2000). Identification of human Rap1:: Implications for telomere evolution. *Cell, 101*(5), 471-483.

Lienhard, G. E. (2008). Non-functional phosphorylations? *Trends in Biochemical Sciences, 33*(8), 351-352.

Lin, S. (2011). Analysis of the role of TRF1 and SMG6 in telomere length maintenance.

Liu, D., Safari, A., O'Connor, M. S., Chan, D. W., Laegeler, A., Qin, J., & Songyang, Z. (2004). PTOP interacts with POT1 and regulates its localization to telomeres. *Nature Cell Biology, 6*(7), 673-680.

Loayza, D., Parsons, H., Donigian, J., Hoke, K., & de Lange, T. (2004). DNA binding features of human POT1. *Journal of Biological Chemistry, 279*(13), 13241-13248.

Makarov, V. L., Hirose, Y., & Langmore, J. P. (1997). Long G tails at both ends of human chromosomes suggest a C strand degradation mechanism for telomere shortening. *Cell, 88*(5), 657.

Martínez, P., Thanasoula, M., Muñoz, P., Liao, C., Tejera, A., McNees, C., . . . Blasco, M. A. (2009). Increased telomere fragility and fusions resulting from TRF1 deficiency lead to degenerative pathologies and increased cancer in mice. *Genes & Development, 23*(17), 2060-2075.

McClintock, B. (1939). The behavior in successive nuclear divisions of a chromosome broken at meiosis. *Proceedings of the National Academy of Sciences of the United States of America, 25*(8), 405.

McClintock, B. (1941). The stability of broken ends of chromosomes in zea mays. *Genetics, 26*(2), 234.

McElligott, R., & Wellinger, R. J. (1997). The terminal DNA structure of mammalian chromosomes. *The EMBO Journal, 16*(12), 3705-3714.

McKerlie, M., & Zhu, X. D. (2011). Cyclin B-dependent kinase 1 regulates human TRF1 to modulate the resolution of sister telomeres. *Nature Communications, 2*, 371.

McKerlie, M. A., Lin, S., & Zhu, X. D. (2012). ATM regulates proteasome-dependent subnuclear localization of TRF1, which is important for telomere maintenance. *Nucleic Acids Research,*

Meyerson, M., Counter, C. M., Eaton, E. N., Ellisen, L. W., Steiner, P., Caddle, S. D., . . . Liu, Q. (1997). < i> hEST2</i>, the putative human telomerase catalytic subunit gene, is up-regulated in tumor cells and during immortalization. *Cell, 90*(4), 785-795.

Meyne, J., Ratliff, R. L., & MoYzIs, R. K. (1989). Conservation of the human telomere sequence (TTAGGG) n among vertebrates. *Proceedings of the National Academy of Sciences, 86*(18), 7049.

Moyzis, R. K., Buckingham, J. M., Cram, L. S., Dani, M., Deaven, L. L., Jones, M. D., . . . Wu, J. R. (1988). A highly conserved repetitive DNA sequence,(TTAGGG) n, present at the telomeres of human chromosomes. *Proceedings of the National Academy of Sciences, 85*(18), 6622.

Muller, H. (1938). The remaking of chromosomes. *Collecting Net, 13*(1), 181-198.

Nakamura, T. M., Morin, G. B., Chapman, K. B., Weinrich, S. L., Andrews, W. H., Lingner, J., . . . Cech, T. R. (1997). Telomerase catalytic subunit homologs from fission yeast and human. *Science, 277*(5328), 955.

Nakanishi, T., Taharas, E., Idez, T., & Ishikawal, F. (1998). Telomerase activation by hTRT in human normal fibroblasts and hepatocellular carcinomas. *Nature Genetics, 18*, 65.

Nishikawa, T., Okamura, H., Nagadoi, A., König, P., Rhodes, D., & Nishimura, Y. (2001). Solution structure of a telomeric DNA complex of human TRF1. *Structure, 9*(12), 1237-1251.

O'Connor, M. S., Safari, A., Xin, H., Liu, D., & Songyang, Z. (2006). A critical role for TPP1 and TIN2 interaction in high-order telomeric complex assembly. *Proceedings of the National Academy of Sciences, 103*(32), 11874-11879.

Ohishi, T., Hirota, T., Tsuruo, T., & Seimiya, H. (2010). TRF1 mediates mitotic abnormalities induced by aurora-A overexpression. *Cancer Research, 70*(5), 2041.

Oikawa, S., Tada-Oikawa, S., & Kawanishi, S. (2001). Site-specific DNA damage at the GGG sequence by UVA involves acceleration of telomere shortening. *Biochemistry, 40*(15), 4763-4768.

Okazaki, R., Okazaki, T., Sakabe, K., & Sugimoto, K. (1967). Mechanism of DNA replication possible discontinuity of DNA chain growth. *Japanese Journal of Medical Science & Biology, 20*(3), 255-260.

Olovnikov, A. (1973). A theory of marginotomy. the incomplete copying of template margin in enzymic synthesis of polynucleotides and biological significance of the phenomenon. *Journal of Theoretical Biology, 41*(1), 181.

Olovnikov, A. M. (1971). Principle of marginotomy in template synthesis of polynucleotides. [Printsip marginotomii v matrichnom sinteze polinukleotidov] *Doklady Akademii Nauk SSSR, 201*(6), 1496-1499.

Palm, W., & de Lange, T. (2008). How shelterin protects mammalian telomeres. *Annual Review of Genetics, 42*, 301-334. doi:10.1146/annurev.genet.41.110306.130350

Poulet, A., Pisano, S., Faivre-Moskalenko, C., Pei, B., Tauran, Y., Haftek-Terreau, Z., . . . Montel, F. (2011). The N-terminal domains of TRF1 and TRF2 regulate their ability to condense telomeric DNA. *Nucleic Acids Research,*

Salazar, C., & Höfer, T. (2007). Versatile regulation of multisite protein phosphorylation by the order of phosphate processing and protein–protein interactions. *FEBS Journal, 274*(4), 1046-1061.

Sarthy, J., Bae, N. S., Scrafford, J., & Baumann, P. (2009). Human RAP1 inhibits non-homologous end joining at telomeres. *The EMBO Journal, 28*(21), 3390-3399.

Sfeir, A., Kosiyatrakul, S. T., Hockemeyer, D., MacRae, S. L., Karlseder, J., Schildkraut, C. L., & de Lange, T. (2009). Mammalian telomeres resemble fragile sites and require TRF1 for efficient replication. *Cell*, *138*(1), 90-103.

Shen, M., Haggblom, C., Vogt, M., Hunter, T., & Lu, K. P. (1997). Characterization and cell cycle regulation of the related human telomeric proteins Pin2 and TRF1 suggest a role in mitosis. *Proceedings of the National Academy of Sciences*, *94*(25), 13618.

Smith, S., & de Lange, T. (1997). TRF1, a mammalian telomeric protein. *Trends in Genetics*, *13*(1), 21-26.

Smith, S., Giriat, I., Schmitt, A., & de Lange, T. (1998). Tankyrase, a poly (ADP-ribose) polymerase at human telomeres. *Science*, *282*(5393), 1484-1487.

Smogorzewska, A., & De Lange, T. (2002). Different telomere damage signaling pathways in human and mouse cells. *The EMBO Journal*, *21*(16), 4338-4348.

Smogorzewska, A., Van Steensel, B., Bianchi, A., Oelmann, S., Schaefer, M. R., Schnapp, G., & De Lange, T. (2000). Control of human telomere length by TRF1 and TRF2. *Molecular and Cellular Biology*, *20*(5), 1659-1668.

Soutoglou, E., Dorn, J. F., Sengupta, K., Jasin, M., Nussenzweig, A., Ried, T., . . . Misteli, T. (2007). Positional stability of single double-strand breaks in mammalian cells. *Nature Cell Biology*, *9*(6), 675-682.

Stansel, R. M., De Lange, T., & Griffith, J. D. (2001). T-loop assembly in vitro involves binding of TRF2 near the 3′ telomeric overhang. *The EMBO Journal*, *20*(19), 5532-5540.

Szostak, J. W., & Blackburn, E. H. (1982). Cloning yeast telomeres on linear plasmid vectors. *Cell*, *29*(1), 245-255.

Takai, K. K., Hooper, S., Blackwood, S., Gandhi, R., & de Lange, T. (2010). *In vivo* stoichiometry of shelterin components. *Journal of Biological Chemistry*, *285*(2), 1457.

Van Steensel, B., & De Lange, T. (1997). Control of telomere length by the human telomeric protein TRF1. *Nature*, , 385,740-743.

van Steensel, B., Smogorzewska, A., & de Lange, T. (1998). TRF2 protects human telomeres from end-to-end fusions. *Cell*, *92*(3), 401-413.

Vannier, J. B., Pavicic-Kaltenbrunner, V., Petalcorin, M. I. R., Ding, H., & Boulton, S. J. (2012). RTEL1 dismantles T loops and counteracts telomeric G4-DNA to maintain telomere integrity. *Cell*, *149*(4), 795-806.

Walker, J. R., & Zhu, X. D. (2012). Post-translational modification of TRF1 and TRF2 and their roles in telomere maintenance. *Mechanisms of Ageing and Development*,

Wang, F., Podell, E. R., Zaug, A. J., Yang, Y., Baciu, P., Cech, T. R., & Lei, M. (2007). The POT1–TPP1 telomere complex is a telomerase processivity factor. *Nature, 445*(7127), 506-510.

Watson, J. D. (1972). Origin of concatemeric T7 DNA. *Nature: New Biology, 239*(94), 197-201.

Wellinger, R., & Sen, D. (1997). The DNA structures at the ends of eukaryotic chromosomes. *European Journal of Cancer, 33*(5), 735-749.

Wright, W. E., Tesmer, V. M., Huffman, K. E., Levene, S. D., & Shay, J. W. (1997). Normal human chromosomes have long G-rich telomeric overhangs at one end. *Genes & Development, 11*(21), 2801-2809.

Wu, Y., Xiao, S., & Zhu, X. D. (2007). MRE11–RAD50–NBS1 and ATM function as co-mediators of TRF1 in telomere length control. *Nature Structural & Molecular Biology, 14*(9), 832-840.

Wu, Z. Q., Yang, X., Weber, G., & Liu, X. (2008). Plk1 phosphorylation of TRF1 is essential for its binding to telomeres. *Journal of Biological Chemistry, 283*(37), 25503-25513.

Xin, H., Liu, D., Wan, M., Safari, A., Kim, H., Sun, W., . . . Songyang, Z. (2007). TPP1 is a homologue of ciliate TEBP-&bgr; and interacts with POT1 to recruit telomerase. *Nature, 445*(7127), 559-562.

Ye, J. Z. S., & de Lange, T. (2004a). TIN2 is a tankyrase 1 PARP modulator in the TRF1 telomere length control complex. *Nature Genetics, 36*(6), 618-623.

Ye, J. Z. S., Donigian, J. R., van Overbeek, M., Loayza, D., Luo, Y., Krutchinsky, A. N., . . . de Lange, T. (2004b). TIN2 binds TRF1 and TRF2 simultaneously and stabilizes the TRF2 complex on telomeres. *Journal of Biological Chemistry, 279*(45), 47264-47271.

Ye, J. Z. S., Hockemeyer, D., Krutchinsky, A. N., Loayza, D., Hooper, S. M., Chait, B. T., & De Lange, T. (2004c). POT1-interacting protein PIP1: A telomere length regulator that recruits POT1 to the TIN2/TRF1 complex. *Genes & Development, 18*(14), 1649-1654.

Zhong, F. L., Batista, L. F. Z., Freund, A., Pech, M. F., Venteicher, A. S., & Artandi, S. E. (2012). TPP1 OB-fold domain controls telomere maintenance by recruiting telomerase to chromosome ends. *Cell, 150*(3), 481-494.

Zhong, Z., Shiue, L., Kaplan, S., & de Lange, T. (1992). A mammalian factor that binds telomeric TTAGGG repeats in vitro. *Molecular and Cellular Biology, 12*(11), 4834-4843.

Zhou, X. Z., Perrem, K., & Lu, K. P. (2003). Role of Pin2/TRF1 in telomere maintenance and cell cycle control. *Journal of Cellular Biochemistry, 89*(1), 19-37.

Zhu, X. D., Kuster, B., Mann, M., Petrini, J. H. J., & de Lange, T. (2000). Cell-cycle-regulated association of RAD50/MRE11/NBS1 with TRF2 and human telomeres. *Nature Genetics, 25*(3), 347-352.

Zhu, X. D., Niedernhofer, L., Kuster, B., Mann, M., Hoeijmakers, J. H. J., & de Lange, T. (2003). ERCC1/XPF removes the 3'overhang from uncapped telomeres and represses formation of telomeric DNA-containing double minute chromosomes. *Molecular Cell, 12*(6), 1489-1498.